



Aerosol mass spectrometry: particle–vaporizer interactions and their consequences for the measurements

F. Drewnick¹, J.-M. Diesch¹, P. Faber¹, and S. Borrmann^{1,2}

¹Max Planck Institute for Chemistry, Particle Chemistry Department, Hahn-Meitner-Weg 1, 55128 Mainz, Germany

²Johannes Gutenberg University, Institute for Atmospheric Physics, J.-J.-Becherweg 21, 55128 Mainz, Germany

Correspondence to: F. Drewnick (frank.drewnick@mpic.de)

Received: 12 February 2015 – Published in Atmos. Meas. Tech. Discuss.: 2 April 2015

Revised: 14 August 2015 – Accepted: 27 August 2015 – Published: 18 September 2015

Abstract. The Aerodyne aerosol mass spectrometer (AMS) is a frequently used instrument for on-line measurement of the ambient sub-micron aerosol composition. With the help of calibrations and a number of assumptions on the flash vaporization and electron impact ionization processes, this instrument provides robust quantitative information on various non-refractory ambient aerosol components. However, when measuring close to certain anthropogenic or marine sources of semi-refractory aerosols, several of these assumptions may not be met and measurement results might easily be incorrectly interpreted if not carefully analyzed for unique ions, isotope patterns, and potential slow vaporization associated with semi-refractory species.

Here we discuss various aspects of the interaction of aerosol particles with the AMS tungsten vaporizer and the consequences for the measurement results: semi-refractory components – i.e., components that vaporize but do not flash-vaporize at the vaporizer and ionizer temperatures, like metal halides (e.g., chlorides, bromides or iodides of Al, Ba, Cd, Cu, Fe, Hg, K, Na, Pb, Sr, Zn) – can be measured semi-quantitatively despite their relatively slow vaporization from the vaporizer. Even though non-refractory components (e.g., NH_4NO_3 or $(\text{NH}_4)_2\text{SO}_4$) vaporize quickly, under certain conditions their differences in vaporization kinetics can result in undesired biases in ion collection efficiency in thresholded measurements. Chemical reactions with oxygen from the aerosol flow can have an influence on the mass spectra for certain components (e.g., organic species). Finally, chemical reactions of the aerosol with the vaporizer surface can result in additional signals in the mass spectra (e.g., WO_2Cl_2 -related signals from particulate Cl) and in conditioning or contamination of the vaporizer, with potential memory ef-

fects influencing the mass spectra of subsequent measurements.

Laboratory experiments that investigate these particle–vaporizer interactions are presented and are discussed together with field results, showing that measurements of typical continental or urban aerosols are not significantly affected, while measurements of semi-refractory aerosol in the laboratory, close to anthropogenic sources or in marine environments, can be biased by these effects.

1 Introduction

Flash vaporization – i.e., very rapid vaporization (here on the order of a few tens of microseconds) of a sample by contact with a hot surface – in combination with mass spectrometry has been used since decades for the analysis of thermally fragile (e.g., Lincoln, 1965; Chinn and Lagow, 1984) or environmental (e.g., de Leeuw et al., 1986) samples with little or no pre-treatment needed. For the measurement of inorganic (e.g., Roberts, 1976; Stolzenburg et al., 2000, 2003) and organic (Lim et al., 2003) aerosol components, flash vaporization is often used in combination with optical gas analyzers. Also in on-line aerosol mass spectrometry flash vaporization was used from the very beginning on in combination with surface ionization (Davis, 1973; Stoffels and Lagergren, 1981) and in later experiments with electron impact ionization (Allen and Gould, 1981; Sinha et al., 1982). Today, one of the most widespread instruments for on-line analysis of the sub-micron aerosol is the Aerodyne aerosol mass spectrometer (AMS), which also applies flash vaporization of the aerosol particles and subsequent electron im-

part ionization of the vapor (Jayne et al., 2000). Common to these applications is the general assumption that flash vaporization quickly converts the solid sample material into a vapor without alteration – besides thermal decomposition – of the sample.

In the AMS the aerosol particles are – together with a small fraction (10^{-7}) of the carrier gas – directed onto the tungsten vaporizer, typically heated to a temperature of 550–600 °C. Non-refractory material flash-vaporizes, and the emerging vapor is electron-impact-ionized (70 eV) for subsequent analysis with a quadrupole (Jayne et al., 2000) or a time-of-flight (Drewnick et al., 2005; DeCarlo et al., 2006) mass spectrometer. In addition to the measurement of the aerosol beam (“beam-open” mass spectrum), also the instrument background is measured with the aerosol beam blocked (“beam-closed” mass spectrum). The particle contribution is calculated from the difference of both measurements (“difference” spectrum), assuming that all particle components vaporize quickly compared to the beam-open–beam-closed cycle length (Jimenez et al., 2003a). For calculation of mass concentrations of species from the difference spectrum, each individual m/z is associated with one or several of these species (Allan et al., 2004b). For the standard analysis of the unit mass resolution spectra, these associations are listed in the “frag table”, which needs to be adapted for special measurement situations by the user. Measurements with the high-resolution time-of-flight AMS (HR-ToF-AMS; DeCarlo et al., 2006) allow the quantification of individual signals in the spectra with certain elemental compositions (Aiken et al., 2007; Canagaratna et al., 2015).

For measurements of the continental or urban background aerosol the assumptions behind this procedure are typically well met and the AMS provides robust quantitative information on the sub-micron aerosol composition (Canagaratna et al., 2007). However, under certain conditions, e.g., when measuring close to anthropogenic sources or in the marine environment, the limitations of these assumptions are sometimes reached and the standard analysis could result in misinterpretation of the mass spectra. Nevertheless, under such conditions additional information extending beyond the standard AMS species can often be retrieved from the mass spectra: in measurements of the marine aerosol, NaCl, which is generally claimed to be refractory and therefore not measurable with the AMS, was unambiguously measured with this instrument (Zorn et al., 2008; Ovadnevaite et al., 2012; Schmale et al., 2013). In the measurements of fireworks (Drewnick et al., 2006) and hand flare emissions (Faber et al., 2013) several metal-containing species (e.g., with Fe, Mg, K, Cu, Li, Na) and their fragments have been identified, albeit not quantified in the mass spectra. Close to a steelworks plant elemental sulfur particles were identified in AMS spectra with the help of collocated single-particle mass spectrometric measurements (Dall’Osto et al., 2012). Finally, during a few AMS measurements in urban environments metals or metal-containing compounds including Rb, Cs, Cu, Zn, As,

Se, Sn, Sb or Pb have been found in the aerosol mass spectra (Takegawa et al., 2009; Salcedo et al., 2010, 2012).

For some of these “unusual” compounds an unusual vaporization behavior was observed with vaporization extending over prolonged time intervals. During the measurement of increased aerosol concentrations, increased background (beam-closed) concentrations have even been observed for the standard non-refractory AMS species (Drewnick et al., 2009; Huffman et al., 2009). For semi-refractory species the background fraction increases (e.g., Salcedo et al., 2010, 2012), sometimes up to a level at which they act as a contamination of the mass spectra, as was observed for bromine and iodine even months after their measurement in the laboratory (e.g., Zorn et al., 2008; Drewnick et al., 2009). In order to extract quantitative information on such species, different approaches have been applied. These include the determination of relative ionization efficiencies (RIEs), either by comparison with external measurements (Drewnick et al., 2006) or by laboratory experiments (Ovadnevaite et al., 2012), or modeling of the mass concentration of a semi-refractory species from the beam-open and beam-closed signals of the mass spectra (Salcedo et al., 2010).

In order to better understand the processes occurring when particles vaporize from the AMS vaporizer, we have performed various experiments in the laboratory. Some of these experiments were focused on the vaporization of individual non-refractory particles; others were focused on the kinetics of particle vaporization of semi-refractory species. In further experiments the influence of the relative humidity (RH) and oxygen in the carrier gas on chemical reactions at the vaporizer was investigated. Additionally, chemical reactions of the aerosol with the vaporizer itself and their influence on the resulting mass spectra have been evaluated. For clarity reasons we divided this manuscript into two main sections, dealing with the kinetics of particle vaporization (Sect. 3) and with chemical reactions at the vaporizer (Sect. 4). Subsequently we discuss the significance of the findings and their potential impact on the measurements in general and for certain measurement conditions.

2 Measurement setup

All laboratory experiments were performed using a similar setup (Fig. 1). Aerosols of known composition were generated by atomizing a solution of the individual components in ultra-pure water (18 M Ω cm, UHQ II, ELGA Purelab) using a constant output atomizer (TSI, model 3076). Subsequently, the aerosol particles were dried in a silica gel diffusion aerosol dryer. For measurements with defined relative humidity the aerosol was passed through a dilution and conditioning chamber, where it was mixed with particle-free air of known RH, resulting in an aerosol RH of 1.5–85 %. For several of the measurements a DMA (differential mobility analyzer, TSI, model 3081) was used to select particles of a

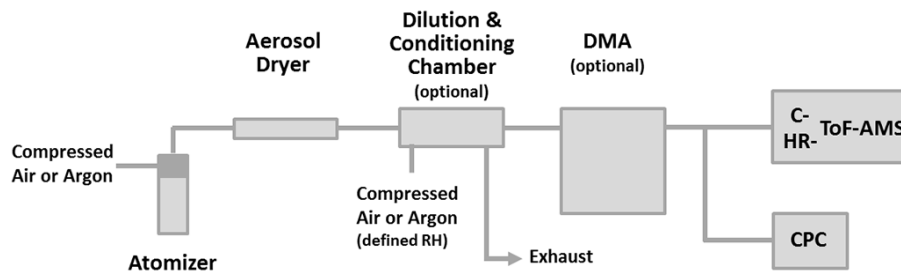


Figure 1. Setup for the measurements of non-refractory and semi-refractory aerosols with defined carrier gas humidity and with air and argon as the carrier gas.

certain diameter or to switch on and off the particle stream without changing any other parameters in the experimental setup. Finally, the aerosol flow was split and directed into the AMS and in parallel into a CPC (condensation particle counter, TSI, model 3025a) for parallel number concentration measurement. In addition, measurements using argon as the carrier and dilution gas were performed to investigate the influence of oxygen in the aerosol upon the resulting mass spectra. In all cases, after changing the carrier gas or the aerosol relative humidity, sufficient time to allow the system to equilibrate (several tens of minutes up to several hours) was given before the measurements under the respective conditions were performed.

All chemicals used for the measurements presented here were of typical analytical purity (97 up to >99 %) and were purchased from several suppliers of laboratory chemicals (Fluka, Carl Roth GmbH, Sigma-Aldrich, and Merck KGaA).

For the aerosol measurements two different aerosol mass spectrometers were used. For the single-particle vaporization event measurements a C-ToF-AMS was applied, which allows very frequent sampling of the ion flow from the vaporizer/ionizer into the mass spectrometer. These measurements were performed with an ion extractor pulser frequency of 83 kHz (1 μ s pulser period) in BFSP mode (brute-force single-particle mode: non-averaged particle time-of-flight (PTOF) mode, i.e., separated collection of a series of consecutive mass spectra without averaging). For all other measurements a HR-ToF-AMS operated in V-mode was used, which does not allow such a high ion sampling rate (pulser frequency of 20 kHz, \sim 50 μ s pulser period) but provides more detailed information on the identity of individual ion peaks from the high-resolution mass spectra. For these measurements mainly the mass spectrum (MS) mode was used. The length of the beam-open and beam-closed cycles varied, depending on the respective type of measurement. If not otherwise stated, measurements were performed with a vaporizer temperature of 600 °C, which was determined using the thermocouple reading of the instrument. Measurements performed with the C-ToF-AMS were analyzed with the data analysis software tool SQUIRREL V1.43; HR-ToF-

AMS data were analyzed using SQUIRREL V1.15H – 1.55D and PIKA V1.10H – 1.14D. For the analysis typical settings and corrections were used; for high-mass resolution analysis multiple ions were added to the PIKA ion list.

3 Particle vaporization kinetics

All AMS measurements are based on the vaporization of individual particles from the AMS vaporizer, a porous tungsten rod with an inverted cone shape (both for improved collection efficiency of the particles), which can be heated up to approximately 800 °C (typical operation temperature: 550–600 °C). When particles impact onto the AMS vaporizer, they can either directly bounce off or remain on the vaporizer. The fraction of bouncing particles ranges between approximately 0 % and more than 50 % and strongly depends on the composition and the phase of the particles, with partially or completely liquid particles showing less bounce than solid particles (Matthew et al., 2008, Middlebrook et al., 2012). Bounced particles are generally assumed to be lost for the analysis and accounted for by applying a collection efficiency correction factor (CE; Canagaratna et al., 2007). Using an AMS equipped with a light-scattering module, delayed particle vaporization events have been observed, which were explained by bounce of particles off the vaporizer and delayed vaporization upon secondary impacts with the vaporizer edges or hot surfaces of the ionizer (Cross et al., 2009). Since we did not find any evidence of vaporization of bounced particles in our experiments, we do not further discuss this possibility here.

Particles which remain on the vaporizer are heated by the hot tungsten surface and, depending on their thermodynamic properties and the vaporizer temperature, can flash-vaporize, vaporize slowly or thermally decompose during the vaporization process. During contact with the vaporizer surface, the hot tungsten could act as a catalyst and support reactions with other aerosol components or with material on the vaporizer surface. Material that leaves the vaporizer as a consequence of the abovementioned processes expands into the ionizer volume, where it can be electron-ionized for subsequent mass spectrometric analysis. Vaporized species as well

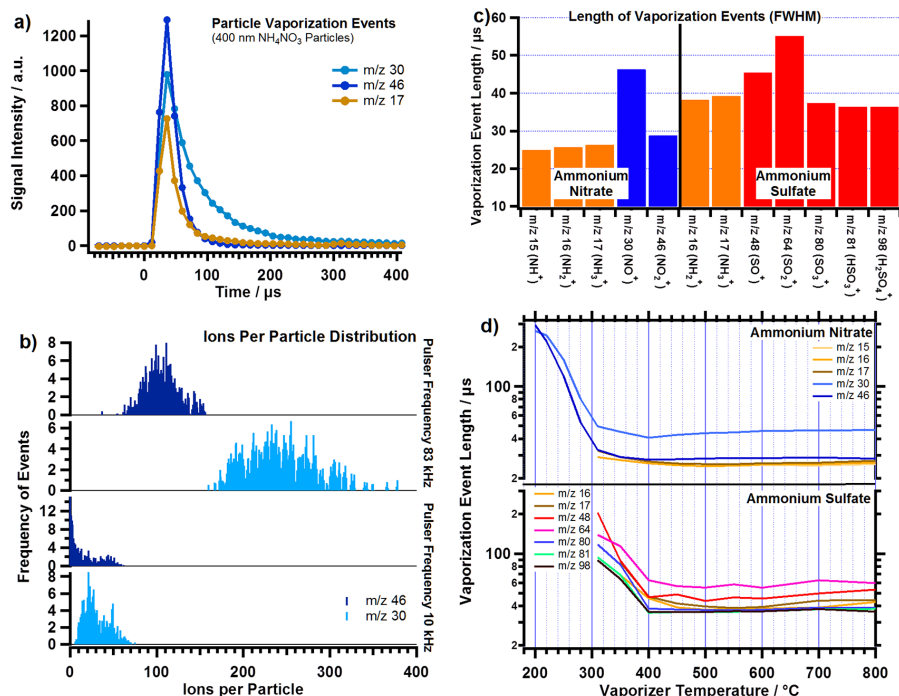


Figure 2. Single-particle vaporization event measurements. **(a)** Average single-particle vaporization events measured for various ions from NH₄NO₃ (ca. 100 events averaged). **(b)** Ions per particle distribution for *m/z* 30 and 46 measured for 400 nm NH₄NO₃ particles with two different ToF-MS pulser frequencies (83 and 10 kHz). **(c)** Vaporization event lengths (FWHM) for ions from NH₄NO₃ and (NH₄)₂SO₄. **(d)** Vaporization event lengths for ions from NH₄NO₃ and (NH₄)₂SO₄ as a function of vaporizer temperature. The uncertainty of event lengths is ~ 10 %. Vaporizer temperature was 600 °C if not otherwise indicated.

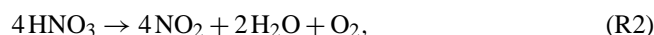
as decomposition products can condense onto surfaces in the ionizer assembly and will desorb, potentially after further decomposition, from these surfaces, depending on the individual temperatures of the respective locations, until they finally end up at sufficiently cool surfaces that they are not desorbed anymore or are removed from the ionizer chamber by the pump. These adsorption–desorption processes can extend the residence time of the respective vapor components according to their tendency to stick to the surfaces (Drewnick et al., 2009).

3.1 Single-particle vaporization events

Ammonium nitrate (NH₄NO₃) and ammonium sulfate ((NH₄)₂SO₄) are the most common inorganic non-refractory species measured with the AMS on a regular basis. Here, single-particle vaporization events for these species have been investigated in some detail in several experiments. For this purpose a C-ToF-AMS was operated at high (83 kHz) pulser frequency in BFSP mode, where measurements on timescales of tens of microseconds are obtained.

In Fig. 2a the typical temporal evolution of ammonium nitrate single-particle vaporization events is depicted for three ions associated with this species, similar to Q-AMS measurements presented by Jayne et al. (2000). The amount of ammonium and nitrate within the particle is proportional to

the integrated area under the peaks related to the respective species. However, in addition to differences in single-particle vaporization event peak area, also differences in peak width and shape can be seen for the three ions. This is likely associated with the thermal decomposition processes occurring during the particle vaporization event (Chien et al., 2010; Ellis and Murray, 1953; Rosser and Wise, 1956):



While in the very early phase of the particle vaporization, when the vapor density is still high, Reaction (R1) as well as the reactions presented further below (Reactions R4–R6) can be assumed to be equilibrium reactions, under the conditions in the AMS they will be very quickly kinetically limited due to the expansion of the evolving vapor from the vaporizer into the surrounding vacuum. Molecules generated during the thermal decomposition processes are ionized by electron impact and as a consequence fragment into the various ions observed in the mass spectra. Within these ions,

m/z 30 (NO^+) is from NO , NO_2 and HNO_3 , while m/z 46 (NO_2^+) is from NO_2 and HNO_3 only (Friedel et al., 1953, 1959). A possible explanation for the longer appearance of the m/z 30 signal – after the other signals already have decayed (Fig. 2a) – is that the NO molecules, as end products of Reactions (R1)–(R3), survive the high-temperature condition longest. Therefore they have the potential to stay longest in the ionizer volume, likely further extended by adsorption–desorption to the ionizer walls. Very sticky molecules like nitric acid and potentially NO_2 are likely removed from the system on the first collision with a cooler surface, prohibiting any extension of their residence time in the ionizer volume by adsorption–desorption processes. If these surfaces have a sufficiently high temperature, thermal decomposition of these molecules with subsequent desorption of decomposition products might occur.

This effect – of the longer single-particle vaporization event length of the m/z 30 ion (46 μs full width at half maximum, FWHM) compared to the m/z 46 ion (29 μs) – can become relevant if the sampling frequency of the ions (i.e., the pulser frequency of the ToF-MS) is small and consequently the pulser period (i.e., the inverse of the pulser frequency) is on the order of the particle vaporization event length. With event lengths on the order of 25–40 μs FWHM for many of the ions, this is the case for measurements with the HR-ToF-AMS (typical pulser periods: 20–40 μs). As a consequence of the less frequent sampling of the ions into the MS, not only is a larger fraction of the ions missed (i.e., the measured number of ions per particle (IPP) is reduced, Fig. 2b), but also the chance to measure only the very small signals in the tails of the vaporization events increases. Since this occurs more frequently for the shorter m/z 46 peak compared to the longer m/z 30 peak, there is a larger chance for m/z 46 not to exceed data acquisition thresholds if they are not set sufficiently low (e.g., in BFSP single-particle measurements, Fig. 2b). This could result in a change in the fragmentation pattern of ammonium nitrate (m/z 30 to m/z 46 ratio) for these single-particle data when the pulser frequency changes, while it should not affect regular averaged AMS measurements. Therefore – and due to the IPP changes – measurements should always be performed with a pulser frequency as high as possible (limited by the desired m/z range of the mass spectra) and at the same pulser frequency as was used during calibration measurements.

For ammonium sulfate, generally slightly longer particle vaporization events are observed, compared to ammonium nitrate (Fig. 2c), both for the sulfate-related ions and for those associated with ammonium. This difference can possibly be explained by the higher temperature needed for quick vaporization of $(\text{NH}_4)_2\text{SO}_4$ compared to NH_4NO_3 , which might result in more time needed to conduct the necessary heat into the particles and potentially slower vaporization kinetics. The even longer vaporization event lengths of the m/z 64 and m/z 48 signals compared to those of m/z 80, 81 and 98 are also associated with the processes during particle vapor-

ization; based on the measured ions in the mass spectra we assume that ammonium sulfate decomposes into ammonia and sulfuric acid under the conditions in the AMS (Reaction R4); sulfuric acid further decomposes and forms SO_3 and SO_2 (Reaction R5 and R6, Wiberg, 2007):



The ions at m/z 81 (HSO_3^+) and 98 (H_2SO_4^+) are only generated from H_2SO_4 , and those at m/z 80 (SO_3^+) from H_2SO_4 and SO_3 , while the ions at m/z 48 (SO^+) and 64 (SO_2^+) are also generated from the emerging SO_2 , which is the final decomposition product according to Reactions (R4)–(R6). An alternative explanation for the longer duration of the vaporization event lengths for m/z 64 and m/z 48 signals compared to those of the other ions could be removal of H_2SO_4 from the system by condensation on cooler ionizer walls followed by slow thermal decomposition and vaporization of the decomposition products instead of re-desorption of the sticky H_2SO_4 molecules. However, also in the early phase of the vaporization events H_2SO_4 makes up only a very small fraction of the vapor molecules, indicating that this species is only a minor fraction of the overall material that leaves the vaporizer. If this small fraction condenses on the ionizer walls and then decomposes and desorbs over extended times, it will contribute only to a very small degree to the overall signal. Therefore we do not assume that slow thermal decomposition of vapor material on the cooler ionizer walls significantly contributes to the lengths of vaporization times.

Flash vaporization assumes “immediate” conversion of a solid or a liquid into a vapor. The finite length of the vaporization events (Fig. 2c) is a consequence of several factors, like the time to heat the whole particle up to a temperature where it vaporizes quickly; the expansion and self-cleaning time constants for the vapor in the ionizer volume, i.e., the time it takes for the vapor to be removed from the ionizer volume, which can be prolonged as a consequence of potential adsorption and desorption processes on the ionizer walls; and ion sampling time constants. Since several of these factors depend on the temperature of the vaporizer, measurements of vaporization event length as a function of vaporizer temperature have been performed.

For low vaporizer temperatures an exponential decrease of vaporization event length with increasing vaporizer temperature is found (Fig. 2d, logarithmic scale). Above a threshold temperature, which depends on the volatility of the species under investigation, no further decrease of vaporization event length with increasing vaporizer temperature is observed.

This threshold temperature is about 310 °C for NH_4NO_3 , 400 °C for $(\text{NH}_4)_2\text{SO}_4$, and 450 °C for NH_4Cl (not shown). In order to be able to measure particle size distributions which are not broadened by slow vaporization of the particles off the vaporizer, its temperature must be set above this threshold value. For example for particle size calibrations, commonly polystyrene latex (PSL) particles are used, which need significantly higher vaporizer temperatures (≥ 750 °C) for sufficiently quick vaporization; in field measurements broadening of size distributions at reduced vaporizer temperatures has also been observed (Docherty et al., 2015). Conversely, this effect can also be used to select the standard AMS vaporizer temperature by setting it to the value at which size distributions of NaNO_3 are just not broadened anymore.

3.2 Vaporization kinetics of non-refractory species

While non-refractory species like ammonium nitrate and ammonium sulfate vaporize quickly and generate short ion pulses when the particles hit the vaporizer, an increase in nitrate or sulfate instrument background with subsequent increase in detection limit for these species has been observed when measuring enhanced concentrations of such aerosol components (Drewnick et al., 2009; Huffman et al., 2009).

To investigate the kinetics of particle vaporization in more detail, experiments have been conducted where the beam-open and beam-closed intervals have been extended way beyond typical operation conditions to approximately 17 min each, and the ion signal was measured during this time with best possible time resolution (~ 5 s, i.e., 1 s sampling time, 4 s saving time; this was the best possible time resolution at the time the measurements were performed). All measurements presented in this section have been performed with 600 °C vaporizer temperature if not otherwise indicated. In Fig. 3a the temporal evolution of the m/z 18 (H_2O^+), 30 (NO^+) and 46 (NO_2^+) signals is shown over three complete beam-open and beam-closed cycles of the measurement of ammonium nitrate particles. While for the nitrate-related ions a very quick increase and decrease of the measured concentrations is observed, the water-related signal shows a slower, more gradual approach to the final levels. In addition, for water even after 17 min of beam-closed measurements still a significant signal background is found ($\sim 56\%$ of signal maximum).

Within the first 10 s of the blocking of the aerosol beam the m/z 30 signal intensity decreases to $\sim 2\%$ of its previous value; for the m/z 46 signal this decrease is even down to $\sim 0.4\%$. During the following 17 min an additional decrease by another factor of 4–5 is observed for both ions. This means that the ratio of m/z 30 to m/z 46 changes from about 2.9 (close to the 3 : 1 ratio of these ions for pure NO_2 ; Friedel et al., 1953) during the aerosol measurement very quickly to a value of 20–25 (i.e., signal dominated by NO) during the background measurement. When the aerosol beam is measured again, the observed signals increase very quickly,

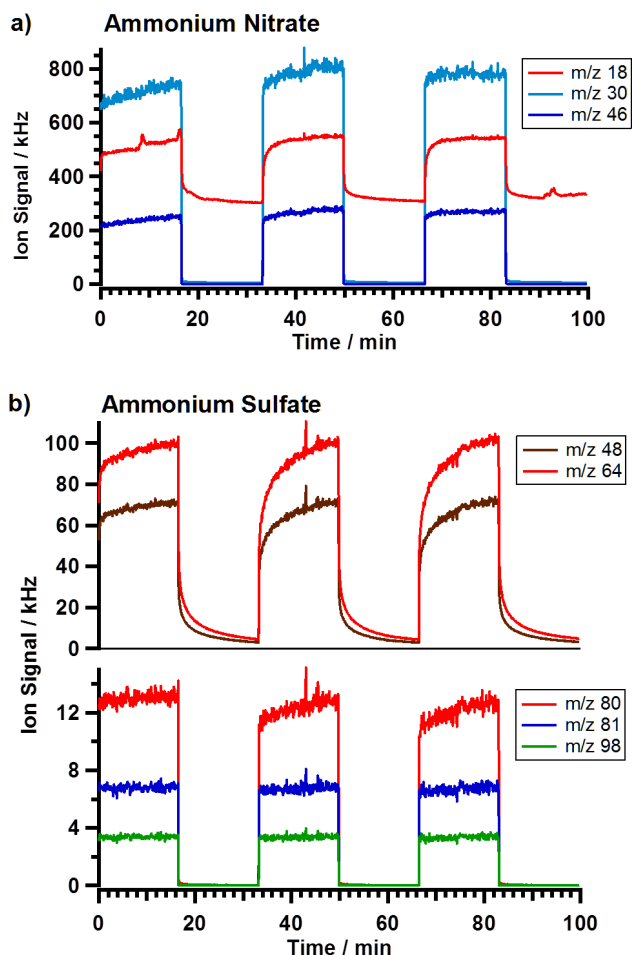


Figure 3. Time-resolved ion signal intensities from measurements of NH_4NO_3 (a) and $(\text{NH}_4)_2\text{SO}_4$ (b) for extended aerosol beam (beam-open) and instrument background (beam-closed) measurements. Precision of the measurements is $< 10\%$; vaporizer temperature was 600 °C.

reaching $\sim 95\%$ of their final value within the first 10 s of measurement. Significantly different behavior is found for the m/z 18 signal, which in parts stems from the thermal decomposition of the nitric acid (Reactions R1 and R2). During the first 10 s of the background measurement this signal decreases to 69 % of its initial value, while it decreases another 13 % during the following 17 min. Also the signal increase after re-opening the particle beam is much slower. After 10 s only 50 % of the previous decrease is recovered.

These results suggest that during the measurement of ammonium nitrate aerosol a small fraction of the nitric acid from the thermal decomposition of the particle material (Reaction R1) is actually ionized and measured in the mass spectrometer, while the majority of the material further decomposes into NO_2 (Reaction R2) before the measurement. As already observed in the single-particle vaporization events, NO_2 quickly decomposes into NO and oxy-

gen (Reaction R3), which causes the domination of NO^+ in the spectra of the instrument background. While the NO is removed from the ionizer volume very quickly, the water background decreases only slowly since the water molecules stick more efficiently to the ionizer walls. Due to the very quick changes in the intensities of the major nitrate-related ion signals when switching on or off the aerosol load, the measured nitrate concentrations, calculated from the difference spectra, do not depend significantly on the length of the beam-open and beam-closed cycles.

The observation of increased ratios of m/z 30 to m/z 46 made for less volatile nitrates (e.g., for KNO_3 we observed a ratio of ~ 28) is completely in line with this picture of the processes on the vaporizer. Since quick vaporization of KNO_3 occurs at higher temperatures compared to NH_4NO_3 , the thermal decomposition, albeit partially along different chemical pathways, progresses further for this species before ionization.

Also for ammonium sulfate the temporal behavior of the measured concentrations was determined for the individual ions with extended beam-open and beam-closed cycle lengths (Fig. 3b). Large differences in the temporal behavior of the signals at m/z 98 (fragment only from H_2SO_4) and m/z 80 and 81 (from H_2SO_4 and SO_3) compared to the signals at m/z 48 and 64 (from H_2SO_4 and SO_3 as well as from SO_2) can be seen. During the first 10 s of aerosol beam blocking, the m/z 48 and 64 signals decrease to $\sim 40\%$ of their initial value; at the end of the 17 min background measurement both signals decrease down to $\sim 4\%$. For the signals at m/z 80, 81, and 98 after 10 s of background measurements the signals are at 2 % for m/z 80 and at 0.3 % for m/z 81 and 98. For m/z 80 a further decrease down to 0.1 % occurs within the following 17 min. Similar behavior is found for the signal increase after restart of the aerosol measurement: for m/z 48 and 64 only $\sim 50\%$ of the total increase in signal occurs within the first 10 s, while for m/z 80, 81, and 98 within the first 10 s already 90 % (m/z 80) and more than 95 % of the final signals are recovered.

These measurements again reflect the very quick thermal decomposition (and vaporization) of ammonium sulfate into ammonia and sulfuric acid (Reaction R4). Only a very small fraction of the sulfuric acid is actually ionized before further decomposition into SO_3 (Reaction R5), which also quickly decomposes into SO_2 (Reaction R6) as indicated by the relative signal intensities and the different temporal behavior of the related ions (Fig. 3b). The slower decay of the m/z 48 and 64 signals suggests that for the SO_2 molecules, which are the end products of the thermal decomposition Reactions (R4)–(R6), the residence times in the ionizer are extended by adsorption–desorption processes at the ionizer walls. Since these two ions contain the dominating fraction of the total sulfate signal, we performed measurements to test whether this slow decay (in relation to the typical beam-open–beam-closed cycle lengths) of the signal causes a dependency of the measured sulfate mass concentration (calculated from

the difference signal) on the length of the measurement cycles (0.5–20 s per half cycle). Compared to the shortest cycle length the signal increased by 5 % when increasing the cycle length up to the maximum value. About 50 % of this increase occurs within the range of cycle lengths from 0.5 up to 5 s. Therefore for typical ranges of measurement cycle lengths (5–10 s) only a change of sulfate measurement efficiency on the order of a few percent must be expected. However, in particle size distribution measurements or single-particle measurements (e.g., for calibration purposes) the time difference between particle signal and instrument background measurement is on the order of a few milliseconds (Canagaratna et al., 2007). Here, a significant reduction in the measured sulfate concentration can be expected compared to a parallel mass concentration measurement (cycle length of a few seconds), which is typically accounted for by scaling the size distribution (PTOF mode) data with mass concentration (MS mode) data.

3.3 Vaporization kinetics of semi-refractory species

The standard AMS target species are sulfate, nitrate, ammonium, chloride and organics. Water also contributes to the AMS mass spectra; however it is typically not quantified due to multiple interferences. Nevertheless, several other species or elements have been observed in measurements performed, e.g., in marine air (Zorn et al., 2008, Ovadnevaite et al., 2012, Schmale et al., 2013) or in urban air (Salcedo et al., 2010, 2012), or in measurements of emissions from pyrotechnical devices (Drewnick et al., 2006; Faber et al., 2013). From our experience, as an empirical proxy, a substance can typically be measured in the AMS with some efficiency if its melting point is not far ($< 200^\circ\text{C}$) above the vaporizer temperature. From comparison of melting (MP) and boiling point (BP) as well as thermal decomposition data (Haynes et al., 2015) with the typical AMS vaporizer temperature (550–600 °C), one can identify substances that can be expected to be measurable with the AMS. We arbitrarily divided these substances into two groups of species which can be expected to be measurable quite well with the AMS (group I, $\text{MP} < 600^\circ\text{C}$ and BP or decomposition temperature $< 900^\circ\text{C}$) and which can be expected to vaporize rather slowly, but still sufficiently fast for detection with the AMS (group II, $\text{MP} < 800^\circ\text{C}$ and BP or decomposition temperature $> 900^\circ\text{C}$). At higher vaporizer temperatures (up to 800°C is possible with the standard vaporizer) these substances can likely be measured more efficiently (albeit with the potential of increased decomposition), and possibly additional substances can be detected with the AMS. A number of metals (mainly the alkali metals) can be expected to be measurable quite well with the AMS in their elemental state (Cd, Cs, Hg, K, Na, Rb, Se; group I). Several others (Al, Ba, Bi, In, Li, Mg, Pb, Te, Tl, Sn, Sr, Zn) belong to group II. For some of these metals their halides probably are harder to vaporize than the pure metals (Cd, Cs, K, Li, Na, Rb), while

Table 1. Overview of elements which can be expected to be measurable in elemental state or as halide, oxide, nitrate, or sulfate with the AMS based on their melting or thermal decomposition points (Haynes et al., 2015). Substances which can be expected to be well measurable with the AMS (group I) are printed in bold; substances which are likely to vaporize slowly but can probably still be measured with the AMS (group II) are printed in normal font.

Chemical compound class	Elements potentially measurable with AMS
Elemental	Al, Ba, Bi, Cd , Cs , Hg , In, K , Li, Mg, Na , Pb, Rb , Te, Tl, Se , Sn, Sr, Zn
Halide	Ag, Al , Au , Ba, Be , Bi , Ca, Cd , Co, Cu, Fe, In , K, Mg, Mo, Na, Os , Pb , Pd , Pt , Rb, Re , Ru , Si , Sn , Sr, Ta , Te , Ti, Tl , V , W , Zn , Zr
Oxide	Ag , Bi , Cs , Hg , K , Os , Pd, Pt , Rb , Re , Ru , Se , Te, Tl
Nitrate	Ag , Al , Ba, Be , Ca, Cd , Cr , Co , Cs, Cu, Fe, Hg , K , Li, Na, Pb, Rb, Sr , Zn
Sulfate	Ag, Co, Cu, Mn, Sn , Ti , V , Zn

for others the halides probably vaporize more easily (Al, Bi, In, Pb, Sn, Te, Tl, Zn). Many metals can only be expected to be measurable in the form of their halides (Ag, Au, Be, Ca, Co, Cu, Fe, Mo, Os, Pd, Pt, Re, Ru, Si, Ta, Ti, V, W, Zr) and not as pure metals. Most of the metal oxides have very high melting points and probably cannot be measured with the AMS, while some others of these substances vaporize (Bi, Cs, Hg, Os, Ru, Se, Te, Tl) or decompose (Ag, K, Pd, Pt, Rb, Re) at sufficiently low temperatures that they might be measurable with this instrument. The nitrates of most metals are likely measurable with the AMS due to their low melting points (several alkali and alkaline earth metals, Ag, Cd, Cu, Pb) or because they decompose at sufficiently low temperature (Al, Cr, Co, Fe, Hg, Zn). Contrarily, the sulfates of the alkali and alkaline earth metals and of Al, Cd, Ni and Pb are likely not measurable with the AMS, while those of some other metals (Ag, Co, Cu, Mn, Sn, Ti, V, Zn) can probably be measured with some efficiency. An overview of substances that can be expected to be measurable with the AMS based on their melting or thermal decomposition points is given in Table 1. Substances belonging to group I are printed in bold, while substances belonging to group II only are printed in normal font.

We have performed a number of laboratory studies focused on the detection of semi-refractory aerosol components, all being metal halides. In Fig. 4a the temporal development of the signal intensity over 25 min of continuous aerosol beam measurement followed by 25 min of instrument background measurement (three repetitions of this cycle) is shown for three ions from the ZnI_2 mass spectrum: m/z 64 (Zn^+), m/z 127 (I^+), and m/z 318 (ZnI_2^+). Apparently ZnI_2 quickly vaporizes from the AMS vaporizer, resulting in an instantaneous increase and decrease of the m/z 318 signal when the particle beam is opened and blocked. Within the first 10 s after blocking the beam, the signal decreases to 0.002 % of its initial value. A quick increase to 80 % of its final value after re-opening the beam is observed within the first 10 s, albeit with an increase of another 20 % over the following 25 min. The m/z 64 (Zn^+) signal reacts significantly slower to changes in the aerosol flow towards the vaporizer, especially when the particle beam is blocked: after 10 s still

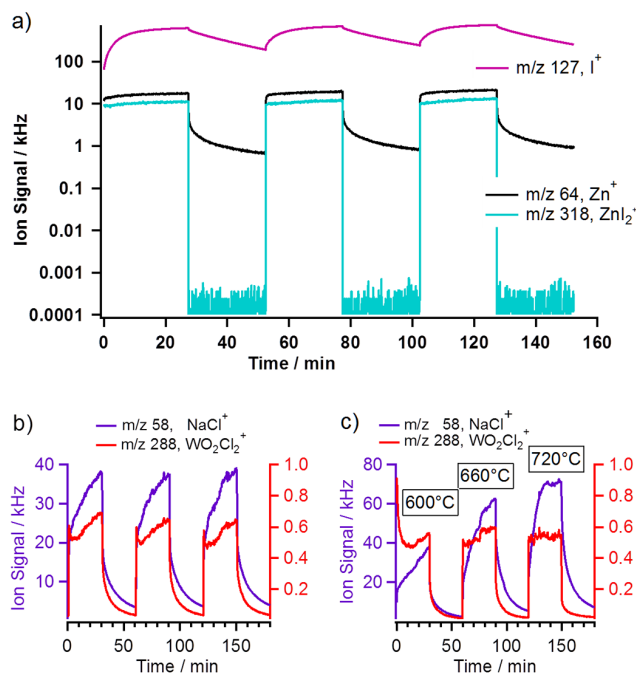


Figure 4. Time-resolved ion signal intensities from measurements of ZnI_2 (a) and NaCl (b, c). In (b, c) the left axis is for NaCl^+ , and the right axis is for WO_2Cl_2^+ . The measurements in (a) and (b) were performed at a constant vaporizer temperature of 600 °C; the measurements in (c) were performed at vaporizer temperatures of 600, 660, and 720 °C. Precision of the measurements is < 10 %.

25 % of the initial signal level is measured, decreasing to 4 % within the following 25 min. After re-opening the aerosol beam 75 % of the signal is re-established within 10 s, further increasing over the following 25 min. The I^+ -related signal (m/z 127) reacts even slower to changes in the aerosol load. Ten seconds after blocking the particle beam, still 92 % of the signal remains in the mass spectra, and after re-opening the beam only 10 % of the final signal is re-established after 10 s. Even during 25 min of background measurement the m/z 64 signal does not drop below 33 % of the value during the aerosol measurement. Apparently, the ZnI_2 quickly vapor-

izes off the vaporizer, with a large fraction of the molecules thermally decomposing. The resulting iodine and zinc efficiently stick to the ionizer walls, where they slowly desorb, causing an increased background signal over extended time intervals. Therefore, for this compound no particle size distribution measurements (where variations of the signal in the range of milliseconds are measured) are possible. For iodine the sticking efficiency is so large that even weeks after such a measurement significant background signal levels are observed (Drewnick et al., 2009). We observed slightly faster decay of this background signal when heating the vaporizer to an elevated temperature for several days.

When the measurement half-cycle lengths are increased from 0.5 to 30 s, the mass concentrations as calculated from the difference signal increase by 50 % for the m/z 64 (Zn^+) and by 80 % for the m/z 127 (I^+) signal, showing that variations in measurement cycle length will have a significant effect on the mass concentrations determined in regular MS mode measurements (difference spectrum with 5–10 s half-cycle length). This mode is based on the assumption that during the beam-open phase the sampled aerosol flash-vaporizes and is measured completely and that during the beam-closed phase only the instrument background is measured. If aerosol-related signals decay slowly over time intervals longer than the half-cycle length, this assumption is not valid anymore. A method to estimate the complete aerosol signal of such substances from the beam-open and beam-closed signals was presented by Salcedo and coworkers (2010).

Results from similar measurements of NaCl are presented in Fig. 4b. For this aerosol component, slow vaporization off and accumulation on the vaporizer are observed. During the 30 min aerosol beam measurement time no stationary state is reached for the vaporization, and during the 30 min background measurement a continuous decay of the NaCl^+ signal is observed down to 20 % of the initial signal intensity. Within the first 10 s after blocking the aerosol beam, the signal decreases by 50 %, and after re-opening the particle beam the signal increases to 40 % of its final level within the same time interval. This slow vaporization of NaCl from the vaporizer makes particle size distribution measurements impossible. When measuring mass concentrations using the regular MS mode, the length of the measurement cycle has an important influence on the calculated mass concentrations: they increase by 22 % when increasing the measurement half-cycle lengths from 0.5 to 30 s.

As shown in Fig. 4c increasing the vaporizer temperature from the standard value (600 °C, used in all measurements if not otherwise specified) to higher temperatures has a strong effect on the kinetics of particle vaporization: the signal increase when opening the particle beam reflects quicker vaporization of the NaCl. At 660 °C the increase levels off much faster during the 30 min of measurement time; at 720 °C a plateau – i.e., a steady state in particle vaporization – is reached after about 8 min of particle measurement.

In addition, even though the aerosol load was kept constant over the whole measurement, the signal intensity increases with increasing vaporizer temperature. The total amount of measured NaCl^+ ions (integrated signal intensity over whole aerosol measurement interval) increases by 75 and 230 % when increasing the vaporizer temperature from 600 to 660 and 720 °C, respectively. At the same time, the more efficient vaporization at elevated vaporizer temperature goes along with a reduced efficiency of ionizer self-cleaning: while at 600 °C vaporizer temperature the signal falls to 45 % of its initial value within 10 s of particle beam blocking, this decrease is only to 65 and 75 % at 660 and 720 °C, respectively. A potential reason for this slower self-cleaning of the ionizer could be that at elevated vaporizer temperatures an increased fraction of the NaCl can also desorb from the ionizer walls which at lower temperatures only act as a sink. Shift of vapor origin would result in longer time constants of NaCl removal due to the lower temperature of the ionizer wall, compared to the vaporizer. In summary, at increasing vaporizer temperature not only the aerosol signal but also, as a consequence of the slower self-cleaning of the ionizer, the beam-closed signal increase. Apparently the increase in beam-closed signal dominates over the increase in measured NaCl^+ ions during the beam-open phase, which results in an overall reduction of the measured NaCl mass concentration (i.e., difference signal), in agreement with the observations of Ovadnevaite et al. (2012).

When aerosol components slowly vaporize or efficiently stick to the ionizer walls and are slowly removed from the ionizer, large instrument background concentrations are the consequence (e.g., Salcedo et al., 2010). The ratio of the signal intensity during the background measurement (beam closed) to the intensity observed when the aerosol beam is measured (beam open), the so-called closed-to-open ratio (c/o), can therefore be used as a proxy for the rapidity at which a certain species vaporizes off the AMS vaporizer and is removed from the ionizer volume. For non-refractory species like ammonium nitrate, c/o is typically on the order of 1 % or even less. Very slowly vaporizing substances have c/o ratios approaching 100 %. In a further set of measurements c/o was determined during measurements of various semi-refractory components. In Fig. 5 c/o is presented for the first 30 min of measurements of $\text{FeCl}_3 \cdot 6 \text{H}_2\text{O}$ (Fig. 5a) and for the first 14 min of measurements of $\text{SrCl}_2 \cdot 6 \text{H}_2\text{O}$ (Fig. 5b). In these experiments the AMS was operated with a vaporizer temperature of 600 °C and a measurement half-cycle length of 7.5 s (beam open and beam closed, each).

Ions resulting from the measurement of iron chloride show very different vaporization behavior (Fig. 5a). The $\text{FeCl}_3\text{NH}_3^+$ signal (probably from partial formation of FeCl_3NH_3 in the particles by reaction with ammonia in the inlet line) has a c/o close to zero, which indicates that this fragment vaporizes very quickly and does not accumulate in the ionizer volume, similarly to FeCl_3^+ , which has a c/o ratio of 2 %. A large degree of accumulation in the ionizer volume builds

Table 2. Relative ionization efficiencies, CE values and c/o ratios for the metals from various metal halides measured during one set of experiments. RIE values were determined with two different approaches (RIE_{pure}, RIE_{mix}). CE values are calculated from the ratio of RIE_{mix} to RIE_{pure}. The measurement uncertainty is $\sim 15\%$ for RIE and $\sim 20\%$ for CE values. For the determination of RIE_{mix}, most species were internally mixed with (NH₄)₂SO₄; only BaCl₂ and SrCl₂ were mixed with NH₄Cl.

	FeCl ₃ · 6H ₂ O	AlCl ₃ · 6H ₂ O	CuCl ₂ · 2H ₂ O	SrCl ₂ · 6H ₂ O	BaCl ₂ · 2H ₂ O	KCl
RIE _{pure}	0.0089	0.0009	0.0242	< 0.0001	< 0.0001	0.0017
RIE _{mix}	0.1584	0.0086	0.2317	0.0005	0.0006	0.0010
CE	0.06	0.11	0.11	0.04	0.03	1.75
c/o_{pure} (%)	12 ± 1	16 ± 3	26 ± 4	79 ± 12	98 ± 3	4 ± 1
c/o_{mix} (%)	20 ± 4	8 ± 1	19 ± 3	98 ± 1	97 ± 5	25 ± 9

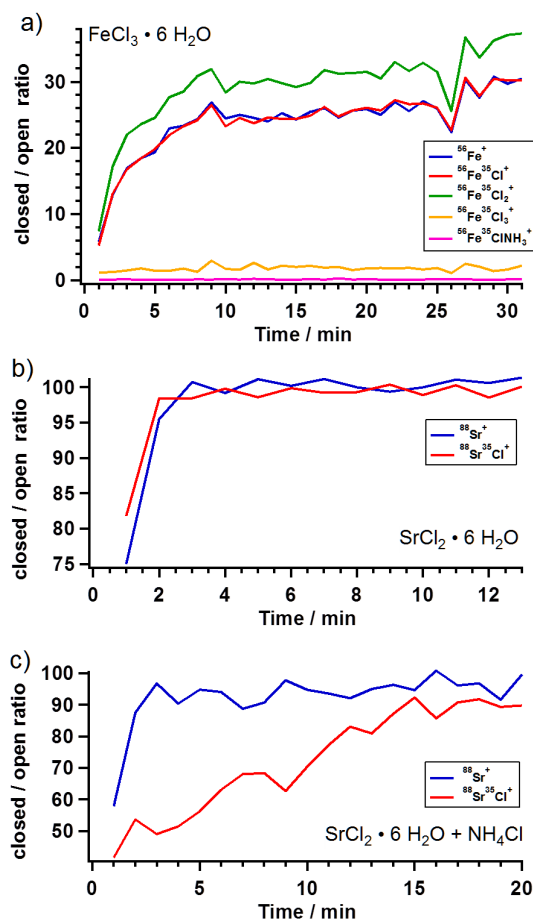


Figure 5. Ratio of instrument background to aerosol beam measurement intensity (c/o ratio, in percent) for ions from FeCl₃ · 6 H₂O (a), from pure SrCl₂ · 6 H₂O (b), and from a mixture of SrCl₂ · 6 H₂O and NH₄Cl (c) for the first minutes of aerosol measurement. Uncertainty of the measurements is $< 15\%$.

up during the first 10 min of measurement for the ions Fe⁺, FeCl⁺ and FeCl₂⁺. This results in c/o ratios of $\sim 32\%$ for FeCl₂⁺ and $\sim 26\%$ for the other two ions, likely as a consequence of slow removal from the ionizer volume because the related molecules stick efficiently to the ionizer walls. The

difference in behavior for these ions suggests that FeCl₃ vaporizes quickly but thermally decomposes into FeCl₂, which sticks sufficiently well to the ionizer walls to cause accumulation in the ionizer volume.

The Sr⁺ and SrCl⁺ ions from the measurement of strontium chloride both show similar vaporization behavior (Fig. 5b). Two minutes after the beginning of the measurement, c/o ratios on the order of 100 % are reached. Apparently SrCl₂ vaporizes very slowly off the vaporizer, resulting in very little difference between the signals during aerosol measurement and background measurement.

In order to obtain quantitative information on aerosol mass concentrations for semi-refractory aerosol components, not only the relative efficiency to ionize the evolved vapor molecules (relative ionization efficiency, RIE) but also the effect of slow vaporization and slow removal from the ionizer volume and consequently high background (beam-closed) signals have to be taken into account. For this purpose we extend the concept of RIE also onto the latter effect. These extended RIE values can be determined in two ways: (1) by comparison of the calculated mass concentration of a test aerosol of pure particles with known particle sizes and number concentrations with its nitrate equivalent mass concentration (the measured mass concentration using RIE = 1), named RIE_{pure}, and (2) by comparison of the measured nitrate equivalent mass concentration of the species with the measured mass concentration of a second species which is internally mixed in the test aerosol at a known ratio, named RIE_{mix}. Generally, any RIE value obtained for semi-refractory components is valid only for the beam-open–beam-closed cycle length and for the vaporizer temperature for which it was determined. The major difference between the two approaches to determine RIE is that RIE_{pure} inherently contains the efficiency of particle collection on the vaporizer (collection efficiency, CE), while RIE_{mix} does not contain CE. Under the assumption that CE is not different for the pure and the mixed particle, the ratio of RIE_{mix} to RIE_{pure} provides the CE value for the respective type of particle. In Table 2 RIE_{pure}, RIE_{mix}, and calculated CE values are provided for a number of semi-refractory species which were investigated in laboratory experiments. In addition the

measured c/o ratios for these species are provided. An alternative quantification method for semi-refractory substances using the beam-open and beam-closed signals was presented by Salcedo et al. (2010).

As expected, the measured RIE values for the semi-refractory species are well below unity. Especially for species with large c/o ratios ($\text{SrCl}_2 \cdot 6 \text{H}_2\text{O}$, $\text{BaCl}_2 \cdot 2 \text{H}_2\text{O}$) very large corrections of the measured mass concentrations are needed to obtain the correct aerosol concentration. All CE values determined from the ratio of the two types of RIE are very low (0.03–0.11), with the exception of the CE value for KCl, which is unrealistically high (1.75). This result shows that the assumption that CE is the same for the pure and the mixed particles is not generally realistic, which was already shown for internally mixed ammonium nitrate and ammonium sulfate particles (Matthew et al., 2008; Middlebrook et al., 2012). Therefore both types of RIE values provide only information on the magnitude of the correction factor needed to obtain realistic aerosol mass concentrations for these semi-refractory species. However, the comparison between RIE values and associated c/o ratios shows that, even though very large c/o ratios are associated with very small RIE values and vice versa, no strict relationship between these two variables is observed. Furthermore, repeated measurements of RIE for $\text{FeCl}_3 \cdot 6 \text{H}_2\text{O}$ over 1 year with multiple other laboratory and field measurements in between have shown that the obtained RIE values (especially RIE_{mix}) are subject to significant changes and apparently depend on the history of the vaporizer (i.e., the “conditioning” by previously measured aerosols). In these measurements an average RIE_{pure} of 0.0061 ± 0.0025 and an average RIE_{mix} of 0.064 ± 0.083 were determined.

Finally, several experiments have provided evidence of matrix effects where as a consequence of chemical reactions of the semi-refractory aerosol component with a matrix component (ammonium) significant changes in vaporization kinetics (i.e., in c/o ratios) were observed, which in turn result in changes in RIE. For the measurements of RIE_{mix} the metal chlorides have been mixed with different ammonium salts in the solution in the atomizer. In the mass spectra, in addition to the signals associated with the salts in the sample, also signals from adduct formation were observed, like $\text{FeCl}_x\text{NH}_3^+$ in the $\text{FeCl}_3/(\text{NH}_4)_2\text{SO}_4$ mixture or $\text{AlCl}_x\text{NH}_3^+$ in the $\text{AlCl}_3/(\text{NH}_4)_2\text{SO}_4$ mixture. Furthermore, we observed shifts in relative signal intensities in the mass spectra of internal mixtures compared to those of pure substances. While in the mass spectra of pure SrCl_2 particles the ion $^{88}\text{Sr}^+$ dominates the spectrum and is about 3 times as intense as the $^{88}\text{Sr}^{35}\text{Cl}^+$ ion, in the mass spectrum of the mixture with NH_4Cl the relation of the intensity of these two signals is approximately inverted. This apparent change in ion generation processes is also reflected in c/o ratios. While for the pure substance both ratios show similar behavior and are on the order of 100% (Fig. 5b), for the

mixtures with ammonium chloride the SrCl^+ signal shows reduced c/o ratios, while that of the Sr^+ signal is largely unchanged (Fig. 5c). Similar behavior was observed for the SO^+ (m/z 48) and SO_2^+ (m/z 64) signals of K_2SO_4 : c/o ratios for both ions were on the order of 30% for the pure substance, while ratios of about 11% were found for these signals in the measurement of mixtures. Apparently, in the mixtures a quicker vaporization of the aerosol substances occurs, compared to the pure substances. In the measurement of FeCl_3 we also observed large changes in the mass spectra when mixtures of FeCl_3 with $(\text{NH}_4)_2\text{SO}_4$ were measured. At constant FeCl_3 concentration in the aerosol an eightfold increase of the $^{35}\text{Cl}^+$ signal was observed in the mass spectra of the mixture, while the intensity of the $^{56}\text{Fe}^+$ signal was reduced by a factor of 6.5, reflecting strong changes in measurement efficiencies for these substances.

Taking all this into account, RIE values for semi-refractory components determined from internal mixtures with other species (RIE_{mix}) should not be generalized for mixtures with different components without further investigation of these effects.

4 Chemical reactions on the vaporizer

The purpose of the vaporizer is to transfer heat to the particles and to induce quick vaporization of the aerosol components. Other interactions between the vaporizer and the particle components, like the initiation of chemical reactions between aerosol components or even chemical reactions between aerosol components and the vaporizer, are not desired. Nevertheless, such reactions occur during aerosol measurements. In the standard AMS analysis procedure (Allan et al., 2004b) particulate chloride is always determined from the signal at m/z 35 ($^{35}\text{Cl}^+$) and 37 ($^{37}\text{Cl}^+$) as well as at m/z 36 (H^{35}Cl^+) and 38 (H^{37}Cl^+). For NH_4Cl the latter ions can be the result of the thermal decomposition process ($\text{NH}_4\text{Cl} \rightarrow \text{NH}_3 + \text{HCl}$), but, since these ions are also observed for other Cl-containing species investigated here (e.g., NaCl or KCl), they are probably also the result of heat-induced chemical reactions of the chlorine with water during the vaporization process. In several measurements, both in the laboratory and in the field, we found evidence of chemical reactions on the vaporizer. Here we present a summary of such findings associated with reactions between aerosol (i.e., particle and carrier gas) components and between aerosol components and the vaporizer.

4.1 Effects of oxygen in the carrier gas

In order to investigate potential chemical reactions of oxygen from the carrier gas with particle components during the measurement with the AMS, experiments have been performed where the same test aerosol, dispersed alternately in air and in argon, was measured. For this purpose the atom-

izer and the dilution and conditioning chamber (Fig. 1) have been operated with argon (> 99.996 %) or dry air (1.5 %RH) until the respective signals in the mass spectra stabilized before the actual aerosol measurement. In these experiments for ammonium nitrate and ammonium sulfate no differences have been observed in the mass spectra with the two different carrier gases.

The degree of oxidation of organic aerosol components is an important piece of information about the age of an aerosol and its degree of atmospheric processing (Jimenez et al., 2009). For this purpose the ratio of oxygen to carbon (O/C ratio) is frequently determined in aerosol analysis. By applying high-resolution elemental analysis to AMS mass spectra of organic aerosols, O/C ratios can be determined with a precision of 5 % (Aiken et al., 2007). In order to test whether O/C ratios measured with the AMS are biased by oxidation of aerosol material during the vaporization process, experiments have been performed where aerosol particles consisting of non-oxygen-containing hydrocarbons (n-hexane, n-decane, polystyrene latex – PSL, and isopropylbenzene) were measured with the AMS, alternately with air and argon as carrier gases and alternately with and without aerosol particles in the carrier gas flow. For measurements with and without the aerosol particles the aerosol was passed through a DMA which was used as a switch for the particles without changing any of the other measurement conditions (Fig. 1).

With the exception of CO_2^+ (m/z 44) no oxygen-containing ions were found in the mass spectra of all four species. Since CO_2^+ is an ion that is also obtained from the air which is analyzed together with the aerosol particles, special care has been taken to separate this “airbeam”-related CO_2^+ from the particle-related CO_2^+ . This was done by calculating the difference of mass spectra with and without aerosol particles (under otherwise unchanged conditions) and by inspecting the PTOF spectra (see Canagaratna et al., 2007), which allow a separation of signal from the airbeam and from the particles.

Using air as the carrier gas, when switching on the aerosol an increase in measured CO_2^+ signal of 14 and 29 % was observed for the aliphatic hydrocarbons n-hexane (C_6H_{14}) and n-decane ($\text{C}_{10}\text{H}_{22}$), respectively. This translates into a fraction of 0.09 % (for n-hexane) and 0.16 % (for n-decane) of the total measured organics concentration. Since the m/z 44 signal is used to calculate organics-related contributions to m/z 16, 17, 18, and 28 (Allan et al., 2004b; Aiken et al., 2008), the overall contribution of this particle-related CO_2^+ signal to the total organics concentration is 0.2 % (n-hexane) and 0.4 % (n-decane). This results in a measured O/C ratio of 0.0016 and 0.003 for n-hexane and n-decane, respectively. Measurements with argon as the carrier gas did not provide clear results since it was not possible to quantitatively replace the air in the carrier gas of the measured aerosol. Additional measurements in the PTOF mode which provide information

on the size distribution of the particles clearly showed that for both hydrocarbons the change in CO_2^+ signals was associated with particle-related CO_2^+ .

Two aromatic hydrocarbons, i.e., polystyrene latex (PSL, $(\text{C}_8\text{H}_8)_n$) and isopropylbenzene (C_9H_{12}), have also been tested for potential oxidation during measurement in the AMS. For PSL an increase in CO_2^+ signal by 55 % compared to the value obtained when measuring particle-free air was observed; for isopropylbenzene an increase of 170 % was found. For PSL this translates into 0.8 % contribution to the total organics signal, which results in a measured O/C ratio of 0.005; for isopropylbenzene the increase of total organics signal is 2.2 %, and consequently the measured O/C ratio is 0.018. Also for these species, PTOF measurements have shown that the observed increase in CO_2^+ ion signal is associated with the aerosol particles. This increase is significantly reduced when argon is used as the carrier gas instead of air. In summary these measurements have shown that organic species can be partially oxidized by oxygen from the remaining carrier gas when the particles are vaporized in the AMS, resulting in increased O/C ratios. However, it must be noted that these increases in O/C ratios are very small compared to the changes or differences typically observed in ambient measurements.

4.2 Effects of carrier gas humidity

To investigate potential reactions of the vaporizing particle material with water vapor from the carrier gas (air), experiments with 1.5 and 85 % relative humidity of the aerosol have been performed by mixing the aerosol from the atomizer with particle-free dilution air of known humidity (Fig. 1). For better reproducibility, before measurements at high RH the whole system has been equilibrated with particle-free high-RH air for at least 3 h, and before measurements at low RH the equilibration time was at least 14 h. Several alternate measurements at low and high aerosol RH were performed with all other measurement conditions unchanged, and differences between the average mass spectra for both RH levels were determined.

For ammonium nitrate a slight increase in relative signal intensity of m/z 46 (NO_2^+) and m/z 63 (HNO_3^+) compared to the base peak at m/z 30 (NO^+) was observed when increasing the aerosol RH from 1.5 to 85 %. The signal at m/z 46 increases by (5.6 ± 10.5) % (average and standard deviation), while the increase of m/z 63 signal is (13 ± 12) %; thus the changes are barely significant. The tendency of increased m/z 46 and 63 signals with increasing aerosol RH reflects that a larger fraction of the nitrate is measured as HNO_3 and possibly NO_2 instead of further decomposition products. A possible explanation could be quenching of the thermal decomposition of HNO_3 (Reaction R2) due to higher abundance of water, which could take up energy from the HNO_3 molecules during vaporization.

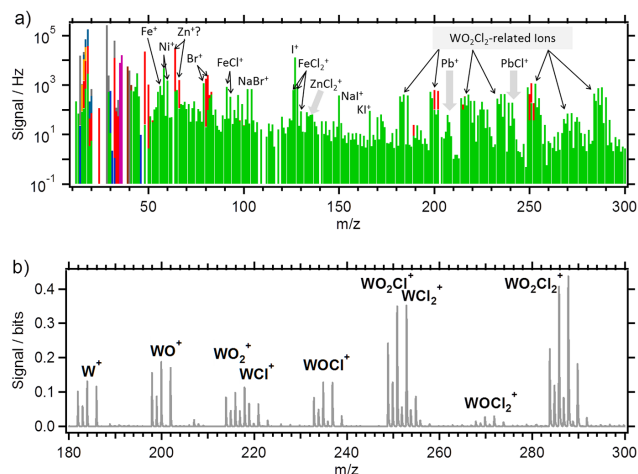


Figure 6. (a) One-minute average unit-mass resolution spectrum from a measurement of the exhaust aerosol of a municipal waste incinerator (ammonium: orange; nitrate: blue; sulfate: red; chloride: purple; organics: green; PAH: also red; association of ion signals from the standard frag table). (b) Cutout of the high-resolution mass spectrum of (a) showing the WO_2Cl_2 -related ion signals.

For ammonium sulfate no significant changes of relative signal intensities (related to the intensity at m/z 64) were found when the aerosol RH was increased from 1.5 to 85 %; for the various ions, average changes of relative signal intensities ranged from -4 up to $+3$ % with an average uncertainty of ± 19 %. Only when correlating the relative signal intensity with the H_2O ionizer background signal (beam-closed m/z 18, H_2O^+ , related to the amount of water introduced into the instrument during recent measurements) was a significant increase in relative m/z 80, 81, and 98 signal intensity with increasing water instrument background level found. From linear regression of the data an increase of $(+38 \pm 18)$ % was found for the m/z 80 signal, of $(+27 \pm 16)$ % for m/z 81, and of $(+28 \pm 17)$ % for m/z 98 over the range of water vapor background signal levels (303–322 kHz) measured within this experiment. These results suggest that also the efficiency of sulfuric acid decomposition is somehow related to the presence of water in the process; however, this dependence results in very small and typically negligible changes in fragmentation patterns.

Experiments with NaCl particles did not show any dependence of the relative intensities of the signals in the associated mass spectra from carrier gas RH; however, the absolute signal intensity increased fourfold when increasing RH from 1.5 to 85 %, likely due to an increase in collection efficiency on the vaporizer, similar to what has been observed for ammonium sulfate in our measurements and previously (Allan et al., 2004a; Matthew et al., 2008).

Table 3. Fragments and isotopes (only W isotopes with > 1 % relative abundance are considered) of tungsten oxide chloride (WO_2Cl_2).

Fragment	Signal at m/z
W^+	182, 183, 184, 186
WO^+	198, 199, 200, 202
WO_2^+	214, 215, 216, 218
WCl^+	217, 218, 219, 220, 221, 223
WOCl^+	233, 234, 235, 236, 237, 239
WO_2Cl^+	249, 250, 251, 252, 253, 255
WCl_2^+	252, 253, 254, 255, 256, 258, 260
WOCl_2^+	268, 269, 270, 271, 272, 274, 276
WO_2Cl_2^+	284, 285, 286, 287, 288, 290, 292

4.3 Chemical reactions with the vaporizer

A 1 min average unit-mass resolution spectrum of the aerosol in the exhaust stack of a municipal waste incinerator measured with a HR-ToF-AMS is shown in Fig. 6a. Besides the typical signals from ammonium, sulfate, nitrate and chloride, also a large number of nominally organics-related signals (green) were found in the spectrum. Since in this aerosol no organic material was expected because of the complete combustion, and due to the unusual patterns of these signals, the high-resolution mass spectrum was inspected in more detail. It turned out that the intense “organics-related” signals in this mass spectrum were associated with bromine, iodine and with halides of potassium, sodium, iron, nickel, zinc and lead. In addition, many intense signals above m/z 180 could be identified as WO_2Cl_2^+ and the various isotopes of the fragments of this ion (Fig. 6b, Table 3). It must be noted that under favorable conditions (i.e., when the contribution to the mass spectrum is sufficiently large) unusual substances could also be identified in unit-mass resolution spectra from their intense signal at m/z where no strong organics-related signals are expected, from isotope patterns or from large background signals, characteristic of semi-refractory substances.

Laboratory experiments with various metal chlorides (AlCl_3 , BaCl_2 , CuCl_2 , FeCl_2 , FeCl_3 , KCl , NaCl , and SrCl_2 , all of which are hydrates except KCl and NaCl ; see Table 2) and with NH_4Cl showed that the occurrence of WO_2Cl_2 signals in the mass spectra is a general feature when measuring Cl-containing aerosol species. Apparently the WO_2Cl_2 in the vapor phase is a result of the reaction of Cl from the particles with the vaporizer surface, likely with WO_3 that is generated by oxidation of the hot tungsten vaporizer surface by oxygen from the aerosol carrier gas (Wiberg, 2007) and accumulates on the vaporizer surface. This observation is consistent with results reported by Jimenez et al. (2003b), who found MoO^+ and MoO_2^+ ions likely from reactions of iodine-containing substances with the AMS vaporizer (which at the time of these measurements was made of molybdenum) during measurements of iodine-containing particles with the AMS.

Table 4. WO₂Cl₂ generation yields (and standard deviations) and fractional contribution to the total mass spectrum for the measurement of various Cl-containing substances.

Substance	WO ₂ Cl ₂ yield in ng m ⁻³ NO ₃ -eq./ μg Cl m ⁻³	WO ₂ Cl ₂ contribution to total mass spectrum
KCl	11.7 ± 1.7	2.7 %
CuCl ₂	7.2 ± 1.0	19 %
FeCl ₃	1.9 ± 0.26	13 %
FeCl ₂	1.7 ± 0.25	15 %
SrCl ₂	0.68 ± 0.09	6.8 %
NaCl	0.40 ± 0.02	0.14 %
AlCl ₃	0.17 ± 0.02	0.15 %
NH ₄ Cl	0.17 ± 0.02	0.04 %
BaCl ₂	0.13 ± 0.01	1.4 %

Strong indications for this process are provided by experiments where the carrier gas was switched between air and argon. Alternate measurements with both types of carrier gases resulted in WO₂Cl₂-related signals about 25 % lower in the measurements with argon, compared to those with air as the carrier gas. In addition, over the course of three argon–air cycles the WO₂Cl₂-related signals decreased more and more. Apparently the WO₃ reservoir at the vaporizer surface got more and more depleted during these measurements. Generally, with increasing Cl concentration in the measured aerosol also the intensities of the WO₂Cl₂-related signals increase. Also for higher vaporizer temperature an increased WO₂Cl₂ signal was observed: in measurements of FeCl₃ aerosol the WO₂Cl₂-related signal, normalized on the Cl signal, increased by a factor of 2 when the vaporizer temperature was increased from 600 to 800 °C. At the same time enhanced fragmentation of the WO₂Cl₂ into preferentially smaller fragments was observed in the measurements at elevated vaporizer temperature. This dependence of WO₂Cl₂ abundance on vaporizer temperature and Cl concentration is in agreement with observations of high-temperature corrosion in industrial systems (Lai, 2007).

Time-resolved data of WO₂Cl₂ from extended aerosol beam-open–beam-closed measurements of NaCl (Fig. 4b, c) provide indications that during the background measurements tungsten from the vaporizer is oxidized, which results in an accumulation of WO₃ at the vaporizer surface. When switching to the aerosol beam measurement, the reaction of the aerosol with the conditioned vaporizer surface causes a spike in measured WO₂Cl₂ signals, which lasts for about 1 min (Fig. 4b). In the following minutes the WO₂Cl₂ signal increases slowly. When argon is used as the carrier gas or at higher vaporizer temperature (Fig. 4c), this WO₂Cl₂ spike at the beginning of NaCl measurements is less pronounced; apparently under these conditions the conditioning of the vaporizer during the background measurement is less efficient. Finally, the genera-

tion of WO₂Cl₂ per amount of Cl in the aerosol depends on the type of aerosol measured; in our experiments we found WO₂Cl₂ yields in the order KCl > CuCl₂ > FeCl₃ ≈ FeCl₂ > SrCl₂ > NaCl > AlCl₃ ≈ NH₄Cl ≈ BaCl₂ (for individual values, see Table 4). For KCl 12 ng m⁻³ NO₃-eq. WO₂Cl₂ was measured per μg Cl m⁻³ expected from the aerosol concentration; this yield was about 90 times larger than that for BaCl₂ (0.13 ng m⁻³ NO₃-eq./μg Cl m⁻³). With a WO₂Cl₂ yield of 0.40 ng m⁻³ NO₃-eq./μg Cl m⁻³, NaCl ranges at the lower end of observed values. The uncertainties of these yields are approximately 15 %. The fractional contribution of the WO₂Cl₂-related signals to the mass spectrum depends both on the yield and on the efficiency of vaporization of the respective species. For the substances investigated here, WO₂Cl₂ contributed between 0.04 % (NH₄Cl) and 19 % (CuCl₂) to the total mass spectra (Table 4). The generation of WO₂Cl₂ signals in the measurement of Cl-containing aerosols is a corrosion process of the vaporizer. Estimating the amount of material removed from the ionizer from the WO₂Cl₂ yields and typical ionization efficiencies shows that the removal of tungsten from the ionizer is completely negligible and that it would take years of continuous measurement of highly concentrated aerosol to remove a single micrometer of the vaporizer material.

Experiments with iron salt aerosols have provided further evidence of chemical reactions at and with the vaporizer surface. As presented above, the RIE (i.e., the efficiency of quick vaporization of a substance) of FeCl₃ particles is affected by the vaporizer history, likely by the resulting surface properties of the vaporizer. In measurements of FeSO₄·7 H₂O no iron-containing signals have been observed, both at 600 and 800 °C vaporizer temperature. The fact that intense sulfate-related signals were found in the mass spectra suggests that FeSO₄ quickly thermally decomposes at the vaporizer surface. Likely Fe is oxidized into Fe₂O₃, which as a refractory component remains on the vaporizer surface. The formation of refractory components on the vaporizer surface is problematic because these processes result in a conditioning of the vaporizer with potential effects on the vaporizer/particle interaction. Exactly this kind of effect was observed in measurements of Fe(NO₃)₃·9 H₂O particles with the AMS: besides intense nitrate-related signals, also small but clear (about 0.1 % of the nitrate-related signals) ion signals of FeCl⁺ (*m/z* 91, 93) and FeCl₂⁺ (*m/z* 126, 128, 130) were observed in the mass spectra. After careful inspection of the whole measurement system and the particle composition, the possibility of contamination of the particles with chlorine can be excluded. Therefore we assume that these ions are the result of chemical reactions between the particle material and chlorine that was bound to the vaporizer as a consequence of previous experiments with Cl-containing particles. This constitutes a memory effect of the AMS vaporizer.

A different type of particle–vaporizer interaction can be observed for potassium-containing particles: due to the low ionization potential of potassium ($E_K = 4.34$ eV) these

atoms can be ionized at the hot tungsten surface (work function $E_W = 4.32\text{--}5.22\text{ eV}$; Haynes, 2015) by surface ionization. Generally, surface ionization is not desired in AMS measurements due to the very intense signals which can be generated by this process and which are not well quantifiable (Allan et al., 2003). In equilibrium, the ratio of the number of potassium ions (n_+) to the number of potassium atoms (n_a) vaporizing from a tungsten surface is a function of the surface temperature T , the work function of tungsten, and the ionization potential of potassium and is described by the Saha–Langmuir equation (Datz and Taylor, 1956),

$$\frac{n_+}{n_a} = \frac{1 - r_+}{1 - r_a} \cdot \frac{1}{2} \cdot \exp\left[\frac{E_W - E_K}{kT}\right], \quad (1)$$

with r_+ and r_a the reflection coefficients for the ion and the atom, respectively. In the AMS, KCl generates the following ions (plus isotopes): Cl^+ (m/z 35), HCl^+ (m/z 36), K^+ (m/z 39), Cl_2^+ (m/z 70), KCl^+ (m/z 74), and K_2Cl^+ (m/z 113). Since the ions from surface ionization are generated at a different location than the ions from electron ionization, they need to follow a different trajectory into the mass spectrometer. In addition to differences in transmission efficiency, this also causes distorted ion peaks in the mass spectra which are shifted to slightly higher m/z (Fig. 7b). Such peak distortions are observed for K^+ but not for KCl^+ and K_2Cl^+ (Fig. 7c). This shows that two different processes occur on the vaporizer: KCl partially vaporizes and in a second step this vapor is ionized by electron impact only; additionally, K atoms occurring at the vaporizer surface can undergo surface ionization with an efficiency depending on the temperature and the work function of the vaporizer, similar to what was observed for NaCl measured with the AMS (Ovadnevaite et al., 2012).

Experiments to investigate the surface ionization process support the abovementioned picture. Since the efficiency of K^+ ions from surface ionization to be transported into the mass spectrometer strongly depends on the setting of the heater bias voltage, this setting was kept constant during these investigations. Measurements of KCl aerosol at different vaporizer temperatures with and without electron impact ionization (filament turned on and off) were performed. When the filament was turned off, at 400°C vaporizer temperature no K^+ signal was observed; i.e., no surface ionization occurred. At 600°C vaporizer temperature strong K^+ ion signals from surface ionization were found; however, when switching on the filament, the K^+ signal increased by a factor of 4, indicating that at this temperature the majority of the K^+ signal stems from electron impact ionization. Finally, at even higher vaporizer temperature (800°C) the vast majority of the K^+ signal originated from surface ionization. Measurements at this vaporizer temperature have shown that the K^+ signal is more than 3 times larger when the filament is turned off compared to the situation with the filament turned on. This result suggests that apparently a large fraction of the ions generated by surface ionization get lost on their way to

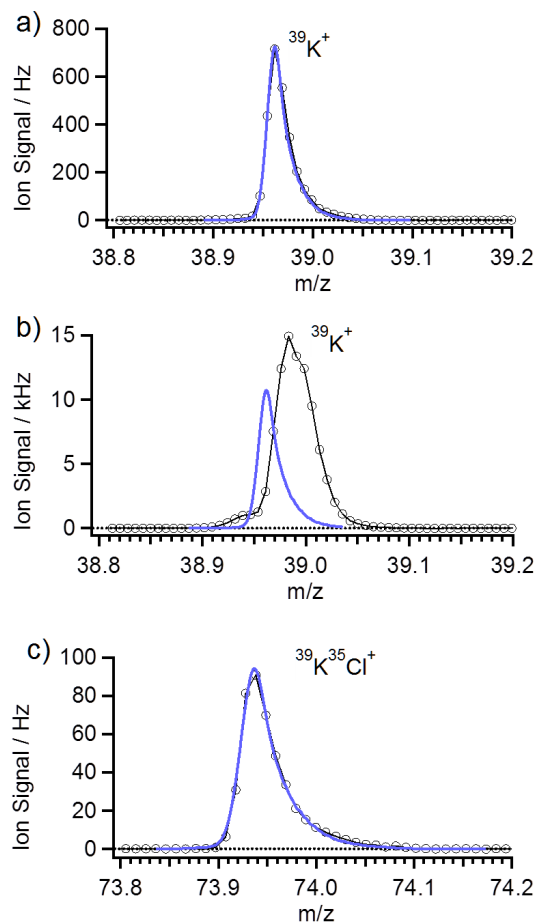


Figure 7. High-resolution mass spectra from the measurement of KCl. Measured data are shown as black markers and traces; blue traces are fits to the data with pre-defined peak positions, shapes and widths according to the expected ion signal. (a) The m/z 39 ($^{39}\text{K}^+$) ion peak at the beginning of the measurement day. (b) The m/z 39 ($^{39}\text{K}^+$) ion peak at the end of the measurement day. (c) The m/z 74 ($^{39}\text{K}^{35}\text{Cl}^+$) ion peak at the end of the measurement day.

the mass spectrometer when the filament is on. This is likely due to associated changes of the electric field in the ionizer volume when the filament is turned on and off, possibly as a consequence of the presence of electrons from the filament in the ionizer volume. This electric field is optimized for detection of ions generated by electron impact ionization at a different location of the ionizer compared to the location where the surface ionization takes place, i.e., the vaporizer surface. Therefore the fraction of ions from surface ionization measured in these experiments is likely below the actually generated fraction of ions.

During the first measurements on a measurement day K^+ ions almost exclusively from electron impact ionization with the regular ion peak shape (Fig. 7a) were observed in the high-resolution mass spectra. After the measurement of several semi-refractory metal chlorides (FeCl_3 , BaCl_2 , SrCl_2 ,

CuCl₂) over the day the measurements with KCl were repeated. While in these measurements no significant changes for the intensity of KCl⁺ and K₂Cl⁺ (both ions only from electron impact ionization) were found, the K⁺ signals were more than 10 times larger compared to the measurement in the morning. The observed increase in relative signal intensity and the changed ion signal peak shape (Fig. 7b) indicate that in these measurements a large fraction of the K⁺ signal is from surface ionization. This change over the course of the day suggests that the vaporizer history has an important influence on the efficiency of surface ionization. Apparently the adsorption of chlorine atoms at the vaporizer surface over the day caused an increase in work function for the tungsten surface (Jowett and Hopkins, 1970), associated with an increase in surface ionization efficiency (Datz and Taylor, 1956).

5 Discussion

Our experiments, in agreement with several previous publications (e.g., Drewnick et al., 2006; Zorn et al., 2008; Salcedo et al., 2010, 2012; Ovadnevaite et al., 2012; Faber et al., 2013) have shown that for measurements with the AMS a sharp separation of species into non-refractory and refractory aerosol components is not valid. The standard AMS species (ammonium nitrate, ammonium sulfate, organics) vaporize very quickly from the AMS vaporizer. Differences in vaporization event lengths were observed for these species which are likely associated with the residence times of various decomposition products in the ionizer. Since these vaporization timescales are often on the order of the extraction pulser periods, single-particle measurements and associated IPP values must be obtained with sufficient particle statistics to accurately capture the average single-particle vaporization event.

Beyond these standard species several other metals; many metal halides, nitrates and sulfates; and a few metal oxides can be measured or can be expected to be measurable with the AMS with some efficiency. From our experience, the melting point of a species can serve as a rough indicator: if it is not well above (approximately 200 °C) the vaporizer temperature, one can expect that the substance can be measured with the AMS. Due to slow vaporization from the vaporizer or efficient adsorption–desorption at the slightly colder ionizer walls, vaporization event lengths for such species can be dramatically extended, from a few tens of microseconds for non-refractory species up to minutes or even more for semi-refractory species. Under such conditions no particle size distribution measurements are possible with the AMS. In addition, such slow vaporization results in a significant fraction of the particle material vaporizing during the phase when nominally the instrument background is measured. This increases the beam-closed/beam-open ratio and as a consequence reduces the difference signal which is used for calculation of particle mass concentrations. In order to obtain quantitative mass concentrations for such species, RIEs which include

the effect of slow vaporization must be determined for each species. While the AMS is generally capable of providing some information on the abundance of such species, quantification with RIE values is possible only to a very limited degree. An RIE value determined for a certain semi-refractory species in the laboratory is only valid for the applied vaporizer temperature and measurement cycle frequency. An alternative quantification method for semi-refractory species using beam-open and beam-closed signals (Salcedo et al., 2010) is less susceptible to these instrumental parameters. Our measurements have shown that RIE values determined for semi-refractory species are also dependent on the particle matrix, i.e., the components internally mixed with the target substance, and on the vaporizer history, i.e., the previous measurements with the instrument. Since these matrix effects also affect *c/o* ratios, the quantification method based on the beam-open and beam-closed signals (Salcedo et al., 2010) could also be impacted by them. Also, since for a given *c/o* very different RIE values are observed, *c/o* alone seems not always to be a sufficient basis for reliable quantification of such species. As a consequence, unless an instrument is carefully calibrated with the species and particle mixtures of interest, such semi-refractory components are only quantifiable with large uncertainties.

While in typical ambient measurements of continental or urban aerosol with the AMS the effects presented here will not measurably affect the determination of the standard AMS species concentrations, under certain conditions they can have significant effects on the obtained mass spectra: in laboratory experiments of aerosols containing semi-refractory material, in measurements close to certain anthropogenic sources or in measurements in the remote marine environment. In measurements in the exhaust of municipal and hazardous waste incinerators we observed strong signals of multiple semi-refractory components like metal halides and WO₂Cl₂ from reaction of particulate Cl with the oxidized vaporizer. Most of these signals were observed at nominally organics-related *m/z*. When the contribution to the mass spectrum is sufficiently large, unusual substances could be identified in unit-mass resolution spectrum from their intense signal at *m/z* where no strong organics-related signals are expected, from isotope patterns or from large background signals, characteristic of semi-refractory substances; in high-resolution mass spectra such species can be readily separated from organics signals. Under conditions where essentially no organic material is in the aerosol (e.g., due to complete combustion) or where very large Cl concentrations occur, ion signals from unusual aerosol components which are not correctly identified by in-depth inspection of the mass spectra can dominate the total mass spectrum and lead to a distorted picture of the aerosol composition. For example during measurements in the remote marine aerosol, WO₂Cl₂, stemming from the very abundant sea salt, was observed, which would have caused an erroneous increase of “organics” mass concentration by 50 % if not correctly interpreted (Zorn, 2009).

From the WO_2Cl_2 yields provided above one can estimate that the ambient particulate Cl concentration must be between 0.6 and 42 times the measured organics concentration in order that the WO_2Cl_2 -related signals exceed the organics contribution to the mass spectrum in the upper m/z range (m/z 180–300). For NaCl particulate chlorine must be 18 times the organics mass concentration.

Especially during laboratory measurements where the exact composition of aerosol components or elemental ratios are desired the possibility of chemical reactions on or with the vaporizer should be taken into account. Experiments have shown that the AMS vaporizer does not always act as an inert vehicle of energy transported to the particles. Chemical reactions of particle components with oxygen in the carrier gas or with components from previous experiments which were accumulated on the vaporizer can result in ion signals in the mass spectra which do not reflect components of the measured aerosol. In principle organic material can be oxidized on the vaporizer and cause positively biased O/C ratios; however, this effect seems to be very small and typically well below the uncertainty of such measurements. In our experiments O/C ratios of non-oxygen-containing species were in the range of 0.0016–0.018. The lowest O/C ratios observed in measurements of ambient aerosol are for hydrocarbon-like organic aerosol (HOA, 0.13) and cooking-related organic aerosol (COA, 0.22), while aged organic aerosol has O/C ratios ranging between 0.50 and 0.85 (Canagaratna et al., 2015).

6 Summary

Various experiments to investigate the interaction of aerosol particles with the vaporizer of the Aerodyne AMS and resulting consequences for the measured mass spectra were conducted. Overall, these investigations show that the AMS vaporizer does not always behave inertly towards the particles and that no sharp separation into non-refractory and refractory components can be made for AMS measurements.

Highly time-resolved measurements of single-particle vaporization events of non-refractory aerosol components (NH_4NO_3 and $(\text{NH}_4)_2\text{SO}_4$) show that above a species-dependent vaporizer temperature threshold vaporization event lengths are on the order of 25–50 μs (FWHM) and do not depend on vaporizer temperature. For certain fragments (NO , SO_2) longer particle vaporization event lengths are observed compared to the other fragments, likely due to a combination of thermal decomposition processes and sticking probabilities to the ionizer wall surfaces. For slow ion extraction frequencies into the mass spectrometer (i.e., for the HR-ToF-AMS) these differences can cause different single-particle measurement efficiencies for the different ions in addition to generally reduced efficiencies. Therefore measurements should generally be performed with the highest possi-

ble ion extraction frequencies of the mass spectrometer and with the same extraction frequencies as used for calibration.

Time-resolved measurements of aerosol and instrument background over extended time intervals provide information on vaporization kinetics for non-refractory and semi-refractory aerosol components. Very quick vaporization of NH_4NO_3 and removal from the ionizer volume cause quick changes in related ion intensities when the aerosol load changes. For $(\text{NH}_4)_2\text{SO}_4$ different behavior is found for different ions: while sulfuric-acid-related ions also show quick changes in intensity, SO_2 -related ion intensities adjust much slower to abrupt changes in aerosol load, likely because they are the end products of the thermal decomposition process and can stick with some probability to the ionizer walls. An alternative explanation for this behavior could be slow thermal decomposition of adsorbed aerosol components on the cooler ionizer walls.

Many metals, metal halides, metal sulfates and metal nitrates vaporize sufficiently fast under the conditions in the AMS and are therefore measurable with some efficiency with this instrument (see Table 1). In order to quantify such semi-refractory species, RIEs have been determined for a number of metal chlorides. As expected, RIE values for these species are well below unity and are very small (<0.001) for species with very large beam-closed/beam-open ratios. As a consequence measured signals have to be multiplied with very large factors in order to obtain ambient mass concentrations. Furthermore, experiments have shown that the RIE values for semi-refractory species do not only depend on vaporizer temperature and measurement cycle length, but can also depend on the aerosol matrix (i.e., the components which are internally mixed with the target species) and the vaporizer history (i.e., previous measurements with the same instrument which can cause conditioning of the vaporizer). Similarly, for KCl the efficiency of surface ionization of potassium was found to be strongly dependent on the vaporizer history. As a consequence of these effects, under general conditions, quantitative measurements of semi-refractory aerosol components are subject to large uncertainties.

Experiments with argon as the carrier gas and with different carrier gas humidities have been performed to investigate possible chemical reactions at the vaporizer. When varying the carrier gas RH, no significant changes in relative peak intensities of ion signals in the mass spectra have been found. In measurements of non-oxygen-containing aliphatic and aromatic hydrocarbons small amounts of oxidation have been observed, resulting in O/C values in the range of 0.0016–0.018, i.e., within the uncertainty of typical ambient O/C ratio measurements.

In addition to chemical reactions of particle and carrier gas components at the vaporizer, also chemical reactions of aerosol components with the vaporizer have been observed. In measurements of Cl-containing species ions of WO_2Cl_2 and its fragments and isotopes can be observed, likely from the reaction of Cl with WO_3 on the vaporizer surface. In other

measurements we observed FeCl^+ and FeCl_2^+ ions during the measurement of $\text{Fe}(\text{NO}_3)_3$, likely from Cl that was accumulated on the vaporizer during previous experiments. In measurements of FeSO_4 only sulfate-related signals have been observed. The iron likely reacted on the vaporizer to Fe_2O_3 , which as a refractory species remains on the vaporizer. Generally, such conditioning of the vaporizer material does not only generate a potential reservoir for ions in mass spectra of future measurements but can also change the “apparent” relative ionization efficiency of some species and thus the efficiency of measurement of these species with the AMS.

While the effects observed in these experiments will not have a significant influence on general ambient measurements of continental or urban aerosols, they can significantly affect the mass spectra under certain conditions like in measurements of laboratory aerosols, probing of anthropogenic sources or in the measurement of remote marine aerosols, when semi-refractory aerosol components can be significant. However, generally such signals from unusual compounds can easily be identified in careful high mass-resolution analysis and accordingly be separated from the organics signals.

Acknowledgements. The authors thank Friederike Freutel for helpful discussions. This work was funded by internal funds of the Max Planck Society. We also thank the two anonymous reviewers for providing many helpful comments which improved the manuscript.

The article processing charges for this open-access publication were covered by the Max Planck Society.

Edited by: P. Herckes

References

- Aiken, A. C., DeCarlo, P. F., and Jimenez, J. L.: Elemental analysis of organic species with electron ionization high-resolution mass spectrometry, *Anal. Chem.*, 79, 8350–8358, 2007.
- Aiken, A. C., DeCarlo, P. F., Kroll, J. H., Worsnop, D. R., Huffman, J. A., Docherty, K. S., Ulbrich, I. M., Mohr, C., Kimmel, J. R., Sueper, D., Sun, Y., Zhang, Q., Trimborn, A., Northway, M., Ziemann, P. J., Canagaratna, M. R., Onasch, T. B., Alfarra, M. R., Prevot, A. S. H., Dommen, J., Duplissy, J., Metzger, A., Baltensperger, U., and Jimenez, J. L.: O/C and OM/OC ratios of primary, secondary, and ambient organic aerosols with high-resolution time-of-flight aerosol mass spectrometry, *Environ. Sci. Technol.*, 42, 4478–4485, 2008.
- Allan, J. D., Alfarra, M. R., Bower, K. N., Williams, P. I., Gallagher, M. W., Jimenez, J. L., McDonald, A. G., Nemitz, E., Canagaratna, M. R., Jayne, J. T., Coe, H., and Worsnop, D. R.: Quantitative sampling using an aerodyne aerosol mass spectrometer, 2, measurements of fine particulate chemical composition in two UK cities, *J. Geophys. Res.-Atmos.*, 108, 4091, doi:10.1029/2002JD002359, 2003.
- Allan, J. D., Bower, K. N., Coe, H., Boudries, H., Jayne, J. T., Canagaratna, M. R., Millet, D. B., Goldstein, A. H., Quinn, P. K., Weber, R. J., and Worsnop, D. R.: Submicron aerosol composition at Trinidad Head, California, during ITCT 2K2: its relationship with gas phase volatile organic carbon and assessment of instrument performance, *J. Geophys. Res.-Atmos.*, 109, D23S24, doi:10.1029/2003JD004208, 2004a.
- Allan, J. D., Delia, A. E., Coe, H., Bower, K. N., Alfarra, M. R., Jimenez, J. L., Middlebrook, A. M., Drewnick, F., Onasch, T. B., Canagaratna, M. R., Jayne, J. T., and Worsnop, D. R.: A generalized method for the extraction of chemically resolved mass spectra from aerodyne aerosol mass spectrometer data, *J. Aerosol. Sci.*, 35, 909–922, 2004b.
- Allen, J. and Gould, R. K.: Mass spectrometric analyzer for individual aerosol particles, *Rev. Sci. Instrum.*, 52, 804–809, 1981.
- Canagaratna, M. R., Jayne, J. T., Jimenez, J. L., Allan, J. D., Alfarra, M. R., Zhang, Q., Onasch, T. B., Drewnick, F., Coe, H., Middlebrook, A., Delia, A., Williams, L. R., Trimborn, A. M., Northway, M. J., DeCarlo, P. F., Kolb, C. E., Davidovits, P., and Worsnop, D. R.: Chemical and microphysical characterization of ambient aerosols with the aerodyne aerosol mass spectrometer, *Mass. Spectrom. Rev.*, 26, 185–222, 2007.
- Canagaratna, M. R., Jimenez, J. L., Kroll, J. H., Chen, Q., Kessler, S. H., Massoli, P., Hildebrandt Ruiz, L., Fortner, E., Williams, L. R., Wilson, K. R., Surratt, J. D., Donahue, N. M., Jayne, J. T., and Worsnop, D. R.: Elemental ratios measurements of organic compounds using aerosol mass spectrometry: characterization, improved calibration, and implications, *Atmos. Chem. Phys.* 15, 253–272, doi:10.5194/acp-15-253-2015, 2015.
- Chien, W.-M., Dhanesh, C., Lau, K. H., Hildenbrand, D. L., and Helmy, A. M.: The vaporization of NH_4NO_3 , *J. Chem. Thermodynamics*, 42, 846–851, 2010.
- Chinn, J. W. and Lagow, R. J.: Characterization of the vapor species of methyl lithium by flash vaporization mass spectrometry, *Organometallics*, 3, 75–77, 1984.
- Cross, E. S., Onasch, T. B., Canagaratna, M., Jayne, J. T., Kimmel, J., Yu, X.-Y., Alexander, M. L., Worsnop, D. R., and Davidovits, P.: Single particle characterization using a light scattering module coupled to a time-of-flight aerosol mass spectrometer, *Atmos. Chem. Phys.*, 9, 7769–7793, doi:10.5194/acp-9-7769-2009, 2009.
- Dall’Osto, M., Drewnick, F., Fisher, R., and Harrison, R. M.: Real-time measurements of nonmetallic fine particulate matter adjacent to a major integrated steelworks, *Aerosol. Sci. Tech.*, 46, 639–653, 2012.
- Datz, S. and Taylor, E. H.: Ionization on platinum and tungsten surfaces, I, the alkali metals, *J. Chem. Phys.*, 25, 389–394, 1956.
- Davis, W. D.: Surface ionization mass spectroscopy of airborne particulates, *J. Vac. Sci. Technol.*, 10, 278, 1973.
- DeCarlo, P. F., Kimmel, J. R., Trimborn, A., Northway, M. J., Jayne, J. T., Aiken, A. C., Gonin, M., Fuhrer, K., Horwarth, T., Docherty, K. S., Worsnop, D. R., and Jimenez, J. L.: Field-deployable, high-resolution, time-of-flight aerosol mass spectrometer, *Anal. Chem.*, 78, 8281–8289, 2006.
- de Leeuw, J. W., de Leer, E. W. B., Sinnighe Damsté, J. S., and Schuyf, P. J. W.: Screening of anthropogenic compounds in polluted sediments and soils by flash evaporation/pyrolysis gas chromatography-mass spectrometry, *Anal. Chem.*, 58, 1852–1857, 1986.
- Docherty, K. S., Lewandowski, M., and Jimenez, J. L.: Effect of Vaporizer Temperature on Ambient Non-Refractory Submicron

- Aerosol Composition and Mass Spectra Measured by the Aerosol Mass Spectrometer, *Aerosol Sci. Tech.*, 49, 485–494, 2015.
- Drewnick, F., Hings, S. S., DeCarlo, P., Jayne, J. T., Gonin, M., Fuhrer, K., Weimer, S., Jimenez, J. L., Demerjian, K. L., Borrmann, S., and Worsnop, D. R.: A new time-of-flight aerosol mass spectrometer (TOF-AMS) – instrument description and first field deployment, *Aerosol Sci. Tech.*, 39, 637–658, 2005.
- Drewnick, F., Hings, S. S., Curtius, J., Eerdekens, G., and Williams, J.: Measurement of fine particulate and gas-phase species during the New Year's fireworks 2005 in Mainz, Germany, *Atmos. Environ.*, 40, 4316–4327, 2006.
- Drewnick, F., Hings, S. S., Alfarra, M. R., Prevot, A. S. H., and Borrmann, S.: Aerosol quantification with the aerodyne aerosol mass spectrometer: detection limits and ionizer background effects, *Atmos. Meas. Tech.*, 2, 33–46, doi:10.5194/amt-2-33-2009, 2009.
- Ellis, W. R. and Murray, R. C.: The thermal decomposition of anhydrous nitric acid vapour, *J. Appl. Chem.*, 3, 318–322, 1953.
- Faber, P., Drewnick, F., Veres, P. R., Williams, J., and Borrmann, S.: Anthropogenic sources of aerosol particles in a football stadium: real-time characterization of emissions from cigarette smoking, cooking, hand flares, and color smoke bombs by high-resolution aerosol mass spectrometry, *Atmos. Environ.*, 77, 1043–1051, 2013.
- Friedel, R. A., Sharkey Jr., A. G., Schultz, J. L., and Humbert, C. R.: Mass spectrometric analysis of mixtures containing nitrogen dioxide, *Anal. Chem.*, 25, 1314–1320, 1953.
- Friedel, R. A., Shultz, J. L., and Sharkey Jr., A. G.: Mass Spectrum of Nitric Acid, *Anal. Chem.*, 31, 1128–1128, 1959.
- Haynes, W. M., Baysinger, G., Berger, L. I., Frenkel, M., Goldberg, R. N., Kuchitsu, K., Roth, D. L., and Zwillinger, D.: *CRC Handbook of Chemistry and Physics*, 95th edn., Internet Version 2015, CRC Press/Taylor and Francis, Boca Raton, FL, USA, 2015.
- Huffman, J. A., Docherty, K. S., Aiken, A. C., Cubison, M. J., Ulbrich, I. M., DeCarlo, P. F., Sueper, D., Jayne, J. T., Worsnop, D. R., Ziemann, P. J., and Jimenez, J. L.: Chemically-resolved aerosol volatility measurements from two megacity field studies, *Atmos. Chem. Phys.*, 9, 7161–7182, doi:10.5194/acp-9-7161-2009, 2009.
- Jayne, J. T., Leard, D. C., Zhang, X., Davidovits, P., Smith, K. A., Kolb, C. E., and Worsnop, D. R.: Development of an aerosol mass spectrometer for size and composition analysis of submicron particles, *Aerosol Sci. Tech.*, 33, 49–70, 2000.
- Jimenez, J. L., Jayne, J. T., Shi, Q., Kolb, C. E., Worsnop, D. R., Yourshaw, I., Seinfeld, J. H., Flagan, R. C., Zhang, X., Smith, K. A., Morris, J. W., and Davidovits, P.: Ambient aerosol sampling using the aerodyne aerosol mass spectrometer, *J. Geophys. Res.-Atmos.*, 108, 8425, doi:10.1029/2001JD001213, 2003a.
- Jimenez, J. L., Bahreini, R., Cocker III, D. R., Zhuang, H., Varutbangkul V., Flagan, R. C., Seinfeld, J. H., O'Dowd, C. D., and Hoffmann, T.: New particle formation from photooxidation of diiodomethane (CH₂I₂), *J. Geophys. Res.-Atmos.*, 108, 4318, doi:10.1029/2002JD002452, 2003b.
- Jimenez, J. L., Canagaratna, M. R., Donahue, N. M., Prevot, A. S. H., Zhang, Q., Kroll, J., DeCarlo, P. F., Allan, J. D., Coe, H., Ng, N. L., Aiken, A. C., Docherty, K. S., Ulbrich, I. M., Grieshop, A. P., Robinson, A. L., Duplissy, J., Smith, J. D., Wilson, K. R., Lanz, V. A., Hueglin, C., Sun, Y. L., Tian, J., Laakso-
nen, A., Raatikainen, T., Rautiainen, J., Vaattovaara, P., Ehn, M., Kulmala, M., Tomlinson, J. M., Collins, D. R., Cubison, M. J., Dunlea, E. J., Huffman, J. A., Onasch, T. B., Alfarra, M. R., Williams, P. I., Bower, K., Kondo, Y., Schneider, J., Drewnick, F., Borrmann, S., Weimer, S., Demerjian, K., Salcedo, D., Cottrell, L., Griffin, R., Takami, A., Miyoshi, T., Hatakeyama, S., Shimojo, A., Sun, J. Y., Zhang, Y. M., Dzepina, K., Kimmel, J. R., Sueper, D., Jayne, J. T., Herndon, S. C., Trimborn, A. M., Williams, L. R., Wood, E. C., Middlebrook, A. M., Kolb, C. E., Baltensperger, U., and Worsnop, D. R.: Evolution of organic aerosols in the atmosphere, *Science*, 326, 1525–1529, 2009.
- Jowett, C. W. and Hopkins, B. J.: Work function changes due to the adsorption of chlorine, bromine and iodine on tungsten single crystal surfaces, *Surf. Sci.*, 22, 392–410, 1970.
- Lai, G. Y.: *High-Temperature Corrosion and Materials Applications*, ASM International, Materials Park, Ohio, USA, 2007.
- Lim, H.-J., Turpin, B. J., Edgerton, E., Hering, S. V., Allen, G., Maring, H., and Solomon, P.: Semicontinuous aerosol carbon measurements: comparison of Atlanta Supersite measurements, *J. Geophys. Res.-Atmos.*, 108, 8419, doi:10.1029/2001JD001214, 2003.
- Lincoln, K. A.: Flash-vaporization of solid materials for mass spectrometry by intense thermal radiation, *Anal. Chem.*, 37, 541–543, 1965.
- Matthew, B. M., Middlebrook, A. M., and Onasch, T.: Collection efficiencies in an aerodyne aerosol mass spectrometer as a function of particle phase for laboratory generated aerosols, *Aerosol Sci. Tech.*, 42, 884–898, 2008.
- Middlebrook, A. M., Bahreini, R., Jimenez, J. L., and Canagaratna, M. R.: Evaluation of composition-dependent collection efficiencies for the aerodyne aerosol mass spectrometer using field data, *Aerosol Sci. Tech.*, 46, 258–271, 2012.
- Ovadaveite, J., Ceburnis, D., Canagaratna, M., Berresheim, H., Bialek, J., Martucci, G., Worsnop, D. R., and O'Dowd, C.: On the effect of wind speed on submicron sea salt mass concentrations and source fluxes, *J. Geophys. Res.-Atmos.*, 117, D1621, doi:10.1029/2011JD017379, 2012.
- Roberts, P. T. and Friedlander, S. K.: Analysis of sulfur in deposited aerosol particles by vaporization and flame photometric detection, *Atmos. Environ.*, 10, 403–408, 1976.
- Rosser Jr., W. A. and Wise, H.: Thermal Decomposition of Nitrogen Dioxide, *J. Chem. Phys.*, 24, 493–494, 1956.
- Salcedo, D., Onasch, T. B., Aiken, A. C., Williams, L. R., de Foy, B., Cubison, M. J., Worsnop, D. R., Molina, L. T., and Jimenez, J. L.: Determination of particulate lead using aerosol mass spectrometry: MILAGRO/MCMA-2006 observations, *Atmos. Chem. Phys.*, 10, 5371–5389, doi:10.5194/acp-10-5371-2010, 2010.
- Salcedo, D., Laskin, A., Shutthanandan, V., and Jimenez, J.-L.: Feasibility of the detection of trace elements in particulate matter using online high-resolution aerosol mass spectrometry, *Aerosol Sci. Tech.*, 46, 1187–1200, 2012.
- Schmale, J., Schneider, J., Nemitz, E., Tang, Y. S., Dragosits, U., Blackall, T. D., Trathan, P. N., Phillips, G. J., Sutton, M., and Braban, C. F.: Sub-Antarctic marine aerosol: dominant contributions from biogenic sources, *Atmos. Chem. Phys.*, 13, 8669–8694, doi:10.5194/acp-13-8669-2013, 2013.

- Sinha, M. P., Giffin, C. E., Norris, D. D., Estes, T. J., Vilker, V. L., and Friedlander, S. K.: Particle analysis by mass spectrometry, *J. Colloid. Interf. Sci.*, 87, 140–153, 1982.
- Stoffels, J. J. and Lagergren, C. R.: On the real-time measurement of particles in air by direct-inlet surface ionization mass spectrometry, *Int. J. Mass Spectrom.*, 40, 243–254, 1981.
- Stolzenburg, M. R. and Hering, S. V.: Method for the automated measurement of fine particle nitrate in the atmosphere, *Environ. Sci. Technol.*, 34, 907–914, 2000.
- Stolzenburg, M. R., Dutcher, D. D., Kirby, B. W., and Hering, S. V.: Automated measurement of the size and concentration of airborne particulate nitrate, *Aerosol. Sci. Tech.*, 37, 537–546, 2003.
- Takegawa, N., Miyakawa, T., Watanabe, M., Kondo, Y., Miyazaki, Y., Han, S., Zhao, Y., van Pinxteren, D., Brüggemann, E., Gnauk, T., Herrmann, H., Xiao, R., Deng, Z., Hu, M., Zhu, T., and Zhang, Y.: Performance of an aerodyne aerosol mass spectrometer (AMS) during intensive campaigns in China in the summer of 2006, *Aerosol. Sci. Tech.*, 43, 189–204, 2009.
- Wiberg, N.: Holleman – Wiberg, *Lehrbuch der Anorganischen Chemie*, Walter de Gruyter, Berlin, Germany, 2007
- Zorn, S. R.: Chemical Composition Measurements of Pristine Aerosols in the Southern Atlantic and Amazonian Regions by Means of On-line Time-of-Flight Aerosol Mass Spectrometry, Dissertation, Johannes-Gutenberg-University, Mainz, Germany, 2009.
- Zorn, S. R., Drewnick, F., Schott, M., Hoffmann, T., and Borrmann, S.: Characterization of the South Atlantic marine boundary layer aerosol using an aerodyne aerosol mass spectrometer, *Atmos. Chem. Phys.*, 8, 4711–4728, doi:10.5194/acp-8-4711-2008, 2008.